

1      **Separation of an upwelling current bounding the Juan  
2      de Fuca Eddy**

3      **Jody M. Klymak<sup>1,2</sup>, Susan E. Allen<sup>3,4</sup>, Stephanie Waterman<sup>3</sup>**

4      <sup>1</sup>School of Earth and Ocean Sciences, University of Victoria, BC, Canada

5      <sup>2</sup>Department of Physics & Astronomy, University of Victoria, BC, Canada

6      <sup>3</sup>Department of Earth, Ocean and Atmospheric Sciences, University of British Columbia, Vancouver, BC,

7      Canada

8      <sup>4</sup>Institute of Applied Mathematics, University of British Columbia, Vancouver, BC, Canada

9      **Key Points:**

- 10     • The shelf break current along Vancouver Island separates downstream of a submarine  
11     bank.
- 12     • Offshore water is drawn onto the shelf and forms a sharp semi-persistent front with  
13     the Juan de Fuca Eddy.
- 14     • The Eddy shows evidence of long residence times, and little evidence of deep-water  
15     origin.

16      **Abstract**

17      Observations of temperature, salinity, and oxygen on the southern Vancouver Island  
 18      shelf show a large-scale exchange of shelf water with offshore water, just offshore of a semi-  
 19      permanent recirculation. ~~The semi-permanent cyclonic recirculation (, often termed the~~  
 20      Juan de Fuca Eddy). ~~The Eddy~~ occupies a region where the shelf widens abruptly in the  
 21      lee of a bank. The water in this Eddy is a mixture of offshore water and water from a buoyant  
 22      coastal current. This water is well-mixed along a mixing line in temperature-salinity space,  
 23      though it retains stratification, and is either rapidly mixed or has a long residence time.  
 24      There is a ~~sharp less than 1-km wide~~ temperature-salinity front on the offshore side of this  
 25      well-mixed water ~~, no more than 1-km wide, and that~~ has no sign of instabilities. The  
 26      clearest evidence of cross-front transport is found during a ~~short~~ tidally resolved survey over  
 27      a bank, ~~and was~~. ~~The transport is~~ due to flows in the cross-bank direction ~~driving large~~  
 28      ~~mixing in that also drive~~ 50-m tall hydraulic jumps. Upstream of the ~~recirculation~~ ~~Eddy~~  
 29      there is an along-shelf current flowing equatorward. However the whole current separates  
 30      from the shelf before reaching the ~~recirculation~~ ~~Eddy~~, in the lee of a bank, and is replaced by  
 31      water from offshore. The separation event was also seen in sea-surface temperatures from  
 32      satellite images as a tongue of cool coastal water that is ejected offshore.

33      **Plain Language Summary**

34      The southern Vancouver Island continental shelf is biologically productive due to high  
 35      nutrient input from the Strait of Juan de Fuca and Salish Sea estuarine system and sub-  
 36      stantial cross-shelf transport due to the complicated topography. Here we present intensive  
 37      sampling of the Juan de Fuca Eddy region. The observations show that below the surface  
 38      mixed layer, the water in the Eddy is low in oxygen, and has undergone substantial vertical  
 39      and lateral mixing. In contrast to previous literature we find that the low oxygen in the  
 40      ~~eddy~~ ~~Eddy~~ is likely because of respiration rather than being pulled from low-oxygen water  
 41      in the California Undercurrent.

42      The observations also show a remarkable flow separation of the equatorward shelf  
 43      current. The current is seen to detach and is pushed offshore. Such events are readily seen  
 44      in satellite imagery, but our observations indicate that the separation extends the depth of  
 45      the water column on the shelf, and that this separation may be partially driven by the local  
 46      bathymetry. The separation is a very strong cross-shelf exchange event, and transports  
 47      substantial nutrient-rich coastal water offshore to drive productivity in the deeper ocean  
 48      adjacent to the continental slope.

49      **1 Introduction**

50      Cross-shelf exchange is important to the health and productivity of continental shelf  
 51      regions, allowing for offshore oxygenated water to be exchanged with nutrient-rich, but  
 52      oxygen-depleted, nearshore water. Cross-shelf transport usually requires ageostrophic flow,  
 53      since geostrophically balanced flow will tend to follow topographic contours, often providing  
 54      a barrier to lateral exchange (Brink, 2016). Mechanisms of cross-shelf exchange include  
 55      internal waves and instabilities in shelf-break fronts. However, these mechanisms can be  
 56      smaller in magnitude compared to intermittent three-dimensional exchange, driven by ed-  
 57      dying, often catalyzed by topographic irregularity (Barth et al., 2000).

58      Here we present detailed *in-situ* observations from the southern Vancouver Island shelf,  
 59      collected in summer 2013, and sampled by a rapid profiling vehicle equipped with a CTD  
 60      and oxygen sensor, supplemented by traditional hydrographic surveys bracketing the high  
 61      resolution observations by a month. The shelf has complicated bathymetry (Fig. 1), with  
 62      a relatively simple 50-km wide shelf poleward of our study site ~~–~~that widens to over 75  
 63      km wide equatorward of La Perouse Bank. The South Vancouver Island Shelf is this wide

64 shelf region, characterized by a number of banks, and finally is incised on the poleward  
 65 equatorward side by the Juan de Fuca eanyonCanyon. Water from the Strait of Juan de  
 66 Fuca flows poleward as a buoyant current that hugs the coast (Thomson et al., 1989; Hickey  
 67 et al., 1991), while shelf water flows equatorward in the summer both forced by local winds  
 68 and via teleconnections with the long, homogenous shelves equatorward off Washington and  
 69 Oregon (Hickey et al., 1991; Thomson & Krassovski, 2015; Engida et al., 2016). Trapped  
 70 between these two currents is a region of relatively homogenous water that has been termed  
 71 the Juan de Fuca Eddy (Freeland & Denman, 1982; Freeland & McIntosh, 1989; Foreman  
 72 et al., 2008; MacFadyen & Hickey, 2010), denoted “EDDY” below.

73 A goal of our study was to understand how the EDDY persists and how it exchanges  
 74 water properties with offshore water. We focus on water deeper than 50m, below the summer  
 75 mixed layer, because this water is trackable with water mass properties, even though the  
 76 EDDY is often studied from the point of view of the surface circulation (MacFadyen & Hickey,  
 77 2010). Past studies have found low oxygen concentrations in the EDDY, and inferred that  
 78 water is upwelled from the California Undercurrent from as deep as 400 m (Freeland &  
 79 Denman, 1982; Dewey & Crawford, 1988). This inference was based on the assumption  
 80 that oxygen is eonservativea conservative tracer, and hence water in the EDDY had to come  
 81 from the oxygen minimum zone found further offshore (Mackas et al., 1987). ~~This lead~~  
 82 ~~to hypotheses that perhaps It was hypothesized that~~ the EDDY was fed by waters being  
 83 drawn up a spur canyon (called the Spur Canyon) via ageostrophic transport from offshore  
 84 to onshore due to low pressure in the EDDY center (Weaver & Hsieh, 1987). Below, we will  
 85 argue that there is no evidence of such transport and that oxygen is likely low because of  
 86 local consumption due to respiration.

87 A second goal of our study was to better understand cross-shore exchange between  
 88 shelf and offshore water. ~~Cross-shore For a two-dimensional topography with along-shore~~  
 89 ~~wind forcing, cross-shore~~ transport is supplied by Ekman layers~~in simple geometries under~~  
 90 ~~wind forcing~~. However, in many locations there is also evidence of eddies, meanders, and  
 91 filaments driving wholesale separation of shelf currents into the deep ocean. ~~These have~~  
 92 ~~been well-studied off California (Strub et al., 1991) where satellite and in-situ observations~~  
 93 ~~show large meanders of coastal upwelling currents leading to coastal water injected into~~  
 94 ~~the offshore domain.~~ Along the Vancouver Island shelf, large ~~filaments or~~ instabilities of the  
 95 coastal current have ~~also~~ been inferred using satellite images (Ikeda & Emery, 1984; Thom-  
 96 son & Gower, 1998). Direct observations of such filaments have been made further to the  
 97 south off Cape Blanco (Barth et al., 2000), and off other coasts (Relvas & Barton, 2005).  
 98 Net cross-shore transport of nutrients and chlorophyll have been found in hydrographic  
 99 surveys off Vancouver Island (Mackas & Yelland, 1999), and associated with mesoscale fea-  
 100 tures in geostrophic velocities and in satellite observations. The mechanisms driving such  
 101 separations are poorly understood, but hypotheses include coastal hydraulics leading to  
 102 along-shore trapping of coastal waves (Dale & Barth, 2001), wind stress curl variations  
 103 (Castelao & Barth, 2007), induced relative vorticity due to stretching of parcels that over-  
 104 shoot their initial isobaths due to a sudden change in downstream bathymetry (D’Asaro,  
 105 1988), and, at this location, non-linear breaking of large-scale meanders due to baroclinic  
 106 instability between the wind-driven current and the California Undercurrent (Ikeda et al.,  
 107 1984; Battean, 1997).

108 In this paper we present observations of water masses on the Southern Vancouver Island  
 109 Shelf collected in 2013 (section 2), presenting the data in a number of ways to highlight the  
 110 important processes, ~~with a~~. ~~We~~ focus on the offshore side of the EDDY region (section 3)  
 111 where we consider the age of the EDDY, the steadiness of the front separating the EDDY  
 112 and the offshore water, properties along the spur canyonSpur Canyon that was believed to  
 113 feed the EDDY, and a large offshore tongue of the shelf-break current and its intrusion into  
 114 the interior. ~~We discuss conclude by discussing~~ the origin of the EDDY and the implications  
 115 of the separating jet (section 4).

116 **2 Site and Methods**

117 The study site was the southern portion of the Vancouver Island Shelf (Fig. 1a), a  
 118 particularly complicated region due to the bathymetry and varied forcing. At the south end  
 119 of the study site is the Juan de Fuca ~~canyon~~Canyon, which feeds dense water into Juan de  
 120 Fuca Strait. This dense water is mixed with fresh water from the Fraser River at the sills and  
 121 archipelagos further inland and fluxes out the Strait again, where it turns poleward along  
 122 Vancouver Island to form the Vancouver Island Coastal Current. The Juan de Fuca Canyon  
 123 has a notable spur canyon (Spur Canyon) ~~–~~ that incises the shelf towards the north into the  
 124 study site (Fig. 1b). The rest of the shelf is punctuated by a series of banks and shallow  
 125 basins. La Perouse ~~bank~~Bank separates the outer shelf from a deeper inner basin and forms  
 126 the poleward boundary off where the shelf widens abruptly south of 48.5 N. Equatorward,  
 127 the shelf widens further, and the shelf break has a series of submarine canyons, in particular  
 128 Nitnat Canyon and Barkley Canyon.

129 We ~~present observations~~use an along/across-shelf co-ordinate system with an origin  
 130 at 48.4°N and 125.6°W, with the across-shelf *x* oriented 39 degrees north of East (Fig. 1b,  
 131 grey/white alternating lines). The projection is Cartesian with a central latitude at 48.4°N,  
 132 which is sufficient for the limited geographic extents discussed here.

133 Observations from La Perouse hydrographic surveys along the LB and LC lines, col-  
 134 lected aboard the *CCGS Tully* from 2013-05-30 to 2013-05-31 (“May”), and 2013-09-07  
 135 to 2013-09-09 (“September”) are used to put finescale observations in context of routine  
 136 hydrographic work in the study region. These lines span the 50 m isobath to deep offshore,  
 137 with casts every 7.5 km across shelf. The data comes from a lowered Seabird 9-11 CTD,  
 138 with an SBE 43 oxygen sensor. ~~Oxygen data have been corrected against bottle casts, and~~  
 139 ~~the CTD corrected for sensor offsets and thermal lags.~~

140 We focus ~~The focus in this paper is~~ on finescale surveys carried out between these  
 141 hydrographic surveys, from 2013-08-21 to 2013-08-30. Data were collected from the *R/V*  
 142 *Falkor* with an AML Oceanographic Moving Vessel Profiler (MVP). Data was collected  
 143 analogously to data collected during similar field campaigns (Klymak et al., 2015, 2016;  
 144 D’Asaro et al., 2018). The MVP was equipped with an AML Oceanographic CTD, and  
 145 a Rinko Oxygen sensor with a 7-s response time foil. The MVP profiled to depths of 200  
 146 m or to within 5 m of the seafloor, whichever was shallower, and dropped at a speed of  
 147 approximately  $3 \text{ m s}^{-1}$ . Data collection took place while the ship cruised at speeds between  
 148 5 and 8 kts, usually at around 6 kts, to enable fine horizontal spacing of the casts, with  
 149 typical spacing of 800 m in deep water, and less in water shallower than 200 m. Data is  
 150 reported for the downcast, which mostly follows a vertical path. The rapid speed of the  
 151 profiling makes the oxygen measurements somewhat coarse, and probably biased due to the  
 152 phase lag of the sensor, so we treat these qualitatively in this paper.

153 Unfortunately, neither vessel had an operational acoustic Doppler profiler during the  
 154 cruises with which to make water velocity measurements.

155 Winds during the cruises were typical for the west coast of Vancouver Island, with  
 156 equatorward upwelling-favorable winds during July and early August (Fig. 2). During the  
 157 finescale survey, and for the week previous, the winds were intermittently downwelling fa-  
 158 vorable. Note that this locale is strongly affected by coastally trapped waves from further  
 159 south, so doming of near-bottom isopycnals often persists despite local wind forcing, and  
 160 takes a finite amount of time to spin down (Thomson & Krassovski, 2015; Engida et al.,  
 161 2016).

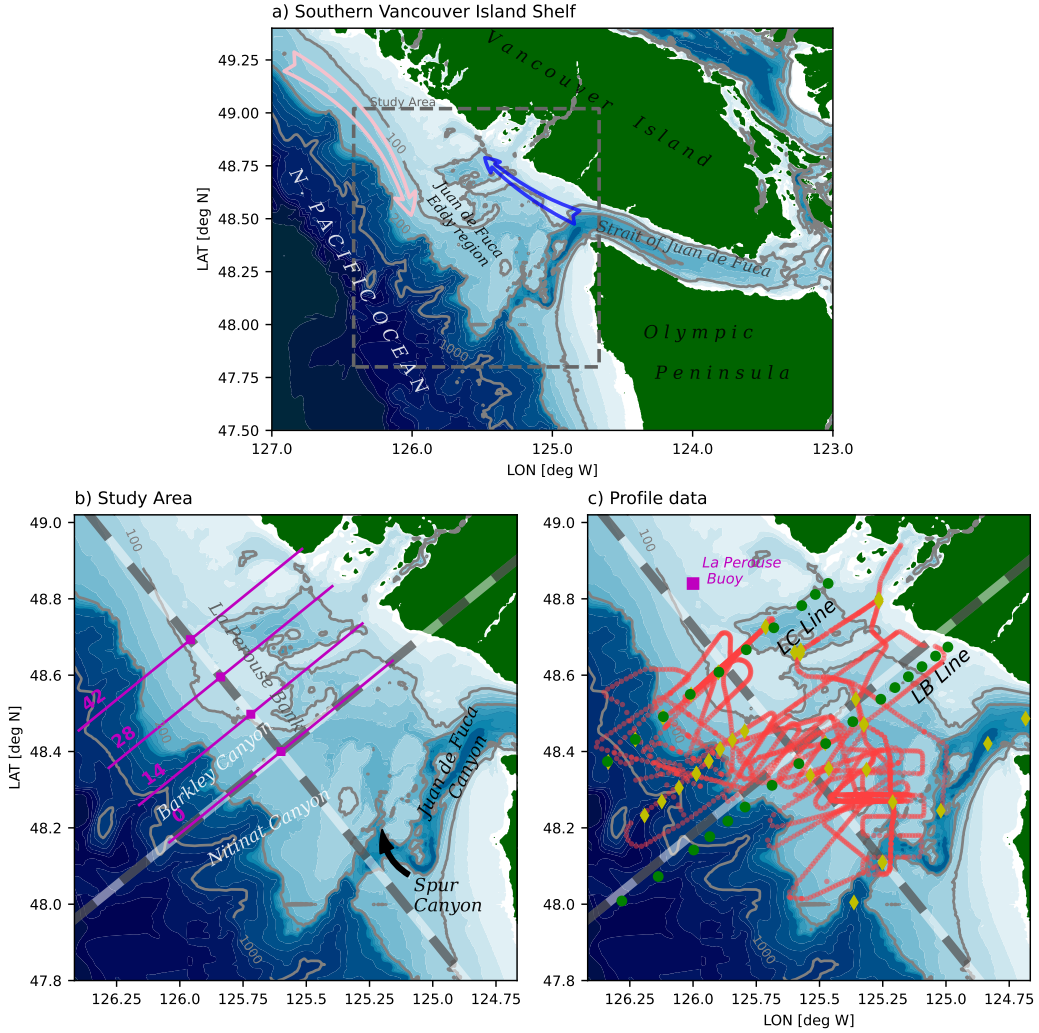


**Figure 1.** a) Study site on the Vancouver Island Shelf. The blue arrow indicates the direction of the Vancouver Island Coastal Current, and the pink arrow indicates southward flow of the coastal upwelling current. The dashed box indicates the approximate limits of the study area. b) The study area with major bathymetric features labelled. The coordinate system used for this paper is shown with alternating grey and white bands at 10-km intervals in the along- and cross-shore directions. c) sample locations with hydrographic casts from the La Perouse cruises along the LB and LC Lines (green dots), hydrographic casts during the Falkor cruise (yellow diamonds), and finescale Moving Vessel Profiler casts (red dots). The coordinate system used for this paper Magenta square is shown with alternating grey and white bands at 10-km intervals in the along- and cross-shore directions La Perouse wind buoy.

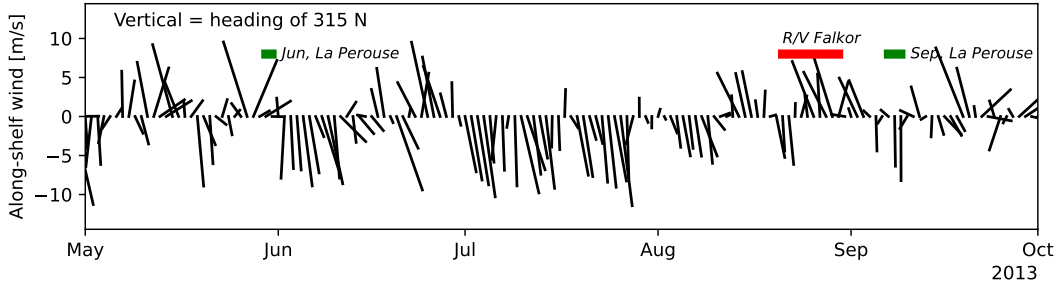


**Figure 2.** Wind from the La Perouse buoy at 48.84 N, 126 W (DFO, 2022). The vertical direction is along-shelf (chosen as a heading of 315 N), so vectors pointing straight down represent upwelling winds. The wind components have been low-pass filtered to one-day averages. The timing of the surveys discussed in the paper are shown as colored bands.

### 3 Observations

#### 3.1 Early and late summer hydrographic surveys

Hydrographic sections along the LB and LC hydrographic lines highlight summer conditions on the Southern Vancouver Island Shelf and indicate some of the features we are focusing on in this paper are presented to give context to the more detailed survey carried out on the *R/V Falkor* (Figure 3). During both surveys, and along both lines, there is clear evidence of upwelling, with the  $26.4 \text{ kg m}^{-3}$  isopycnal reaching from 130 m depth offshore to shallower than 85 m over the shelf. This upwelled water tends to be low in oxygen and cool. Further onshore, the Vancouver Island Coastal Current hugs the coast, where isopycnals tilt down towards the shore, and water is warmer than offshore.

The Juan de Fuca Eddy region is observed along the LB Line (Fig. 3, bottom three rows), mostly inshore of 0 km. This water is cooler and lower in oxygen than along the same isopycnal further offshore. Near the surface, the isopycnals are domed, and the low-oxygen anomaly extends as high as the thin surface mixed layer.

The water upstream of the EDDY region, along the LC line, is less mixed and has higher oxygen than the EDDY water (Fig. 3, top three rows). It does not show as much drawdown of oxygen, and is warmer, at least offshore of La Perouse bank ( $X \approx 5 \text{ km}$ ). Based on these properties, offshore water does not appear to make it over La Perouse bank into the onshore basin, or if it does, it does so intermittently and with substantial mixing. Note that the water along the  $26.4 \text{ kg m}^{-3}$  isopycnal (Fig. 3, magenta contours) becomes cooler and lower in oxygen where it intersects the shelf, consistent with both enhanced mixing near the shelf and with drawdown of oxygen by respiration.

The contrast in onshore and offshore waters can be clearly traced in temperature-salinity ( $\theta-S$ ) anomalies along isopycnals (Fig. 4a). Denser than  $26.6 \text{ kg m}^{-3}$ , the deep water masses found offshore are largely homogenous. In the lighter water masses, there are distinct differences between warm and salty offshore water compared to water on the shelf at the same densities.

We use a spice anomaly defined as relative to a straight line in  $\theta-S$  space (Fig. 4) representing an approximate mixing line for water in the EDDY, and passing through the points  $7.75^\circ\text{C}$ , 30 psu and  $6.6^\circ\text{C}$ , 35 psu. Spice anomaly for a given water sample at density  $\sigma_\theta$  is given by  $\gamma = \alpha(T - T_0(\sigma_\theta)) + \beta(S - S_0(\sigma_\theta))$  where  $T_0(\sigma_\theta)$ ,  $S_0(\sigma_\theta)$  are the temperature and salinity along the mixing line at the same density as the water sample.

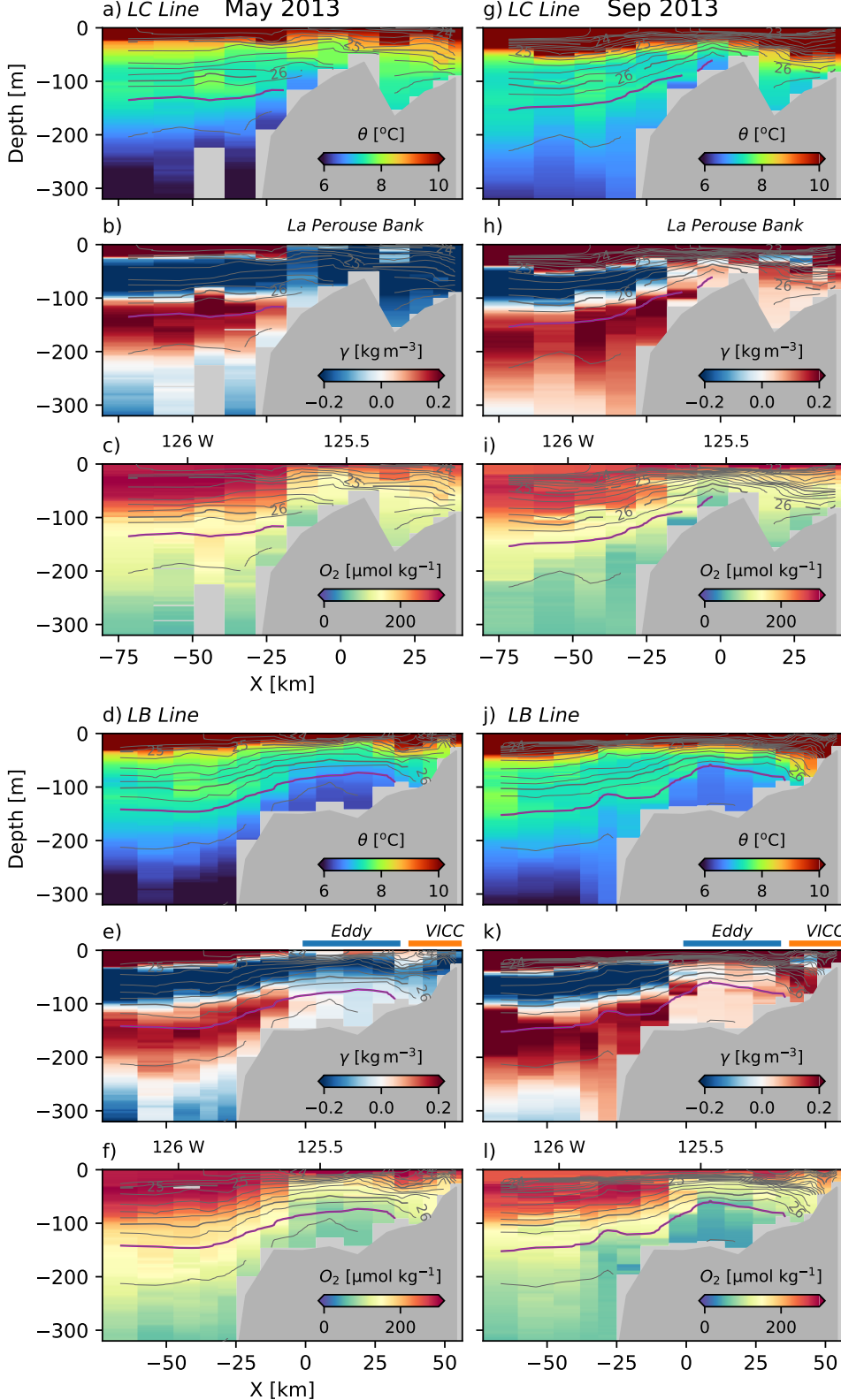


**Figure 3.** Observations along LC Line in May (a–c) and Sep (g–i) and LB lines in May (d–f) and Sep (j–l). X is across-shelf distance in the coordinate system shown in Fig. 1. Potential density is contoured every 0.2 kg m<sup>-3</sup>, with the 26.4 kg m<sup>-3</sup> colored magenta. Potential temperature,  $\theta$ , splice anomaly,  $\gamma$  and oxygen concentration,  $O_2$ , are colored for each section.

194 The sign convention is that a positive anomaly is warmer and saltier than data along the  
 195 mixing line.

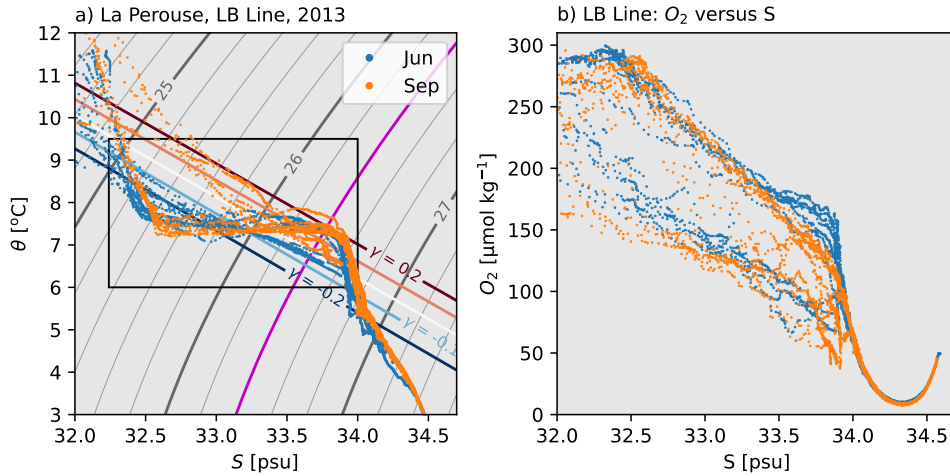


**Figure 4.** a) Potential temperature,  $\theta$ , versus salinity,  $S$ , for the La Perouse data shown in Fig. 3; potential density is contoured every  $0.2 \text{ kg m}^{-3}$ , with the  $26.4 \text{ kg m}^{-3}$  colored magenta. A definition of spice anomaly is shown in this plot, and discussed in the text. The rectangle is the  $\theta - S$  range used in Fig. 5 below. b) The same data with oxygen concentration versus salinity.

196 Using this metric of spice anomaly, offshore water tends to have high absolute values  
 197 (Fig. 3, middle rows), with a positive-anomaly layer ( $\gamma \approx 0.2 \text{ kg m}^{-3}$ , red colors) centered  
 198 at  $26.4 \text{ kg m}^{-3}$  sandwiched between negative-anomaly layers above and below. On the shelf  
 199 ( $-10 \text{ km} < X < 30 \text{ km}$ ), the distinct  $\theta - S$  masses are attenuated and much closer to the  
 200 defined mixing line than the offshore water (closer to white in color in  $\gamma \approx 0 \text{ kg m}^{-3}$ , almost  
 201 white Fig. 3).

202 There are temporal changes over the summer. Away from the surface, water has  
 203 upwelled from deeper depths by September, but the offshore water maintains the same water  
 204 mass characteristics through the summer. Hugging the coast ( $X > 30 \text{ km}$ ), the Vancouver  
 205 Island Coastal Current warms during the summer, and the spice anomaly goes from negative  
 206 to positive. In the EDDY, the water stays near the mixing line, but is cooler in the spring  
 207 (Fig. 3, LB Line, left-hand column: slightly negative spice anomaly) and warms during the  
 208 summer (Fig. 3, LB Line, right-hand column: slightly positive spice anomaly).

209 Oxygen concentration in both surveys has a similar dichotomy between the EDDY and  
 210 off-shelf water. Water found in the EDDY has oxygen concentrations  $100 \mu\text{mol kg}^{-1}$  lower  
 211 on the shelf than off-shelf (Fig. 3, Fig. 4b). The very deepest water ( $S \approx 33.9 \text{ psu}$ ) on the  
 212 shelf shows a further  $50 \mu\text{mol kg}^{-1}$  decrease in concentration between May and September  
 213 along the LB line.

### 214 3.2 Finescale surveys

#### 215 3.2.1 Overview

216 The finescale surveys covered most of the EDDY region, with an emphasis on the  
 217 offshore edge near the shelfbreak front (Fig. 1). For water denser than  $26 \text{ kg m}^{-3}$ , there  
 218 are three distinct water masses sampled on the shelf (Fig. 5). The first is offshore water,  
 219 which tends to be warmer, and hence has a positive spice anomaly ( $\gamma \approx 0.2 \text{ kg m}^{-3}$  along

$\sigma_\theta = 26.4 \text{ kg m}^{-3}$ ). The second is water in the EDDY, which during this survey was found along the straight mixing line in  $\theta - S$  space (Fig. 5,  $\gamma \approx 0 \text{ kg m}^{-3}$  along  $\sigma_\theta = 26.4 \text{ kg m}^{-3}$ ). Between these two water masses, there is a less populous mass (Fig. 5,  $\gamma \approx 0.1 \text{ kg m}^{-3}$  along  $\sigma_\theta = 26.4 \text{ kg m}^{-3}$ ) that we demonstrate below is found on the shelf poleward of the EDDY.

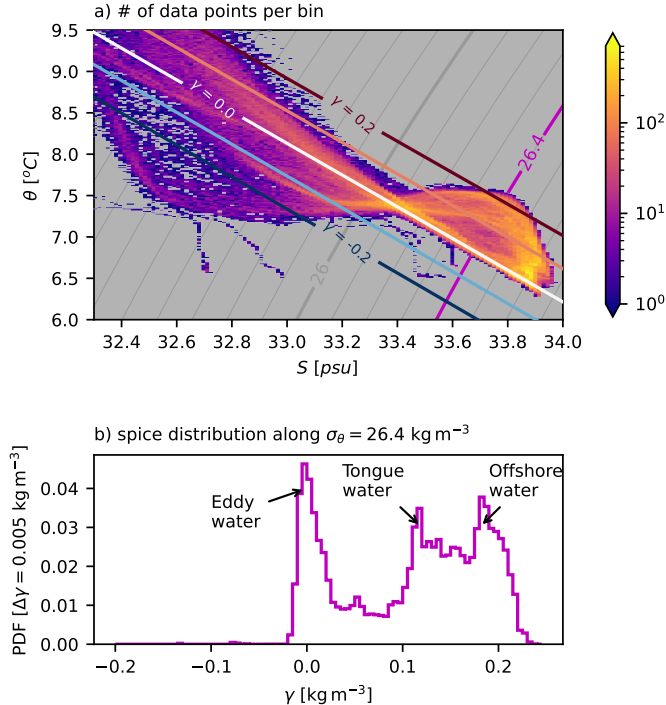


**Figure 5.** a) Binned sample density of salinity and potential temperature from the cruise, with a logarithmic color scale. Grey contours are potential density relative to the surface at intervals of  $0.1 \text{ kg m}^{-3}$ ; the magenta contour is the  $26.4 \text{ kg m}^{-3}$  isopycnal. Colored contours are spice anomaly,  $\gamma$ , relative to the white line labeled  $\gamma = 0.0$ . b) Distribution of spice,  $\gamma$  along the  $26.4 \text{ kg m}^{-3}$  isopycnal.

In synthetic cross sections of spice anomaly, the EDDY is clearly identifiable as having low spice anomaly ( $\gamma \approx 0 \text{ kg m}^{-3}$ , Fig. 6c, d). This signature of well-mixed water extends from the seafloor to approximately 30 m depth, onshore of  $X \approx 0 \text{ km}$ . Despite lying along a mixing line, the EDDY water is still stratified. The high-spice water ( $\gamma \approx 0.2 \text{ kg m}^{-3}$ ) is found offshore of the EDDY water, on the other side of a sharp  $\theta - S$  compensated front. This front is even sharper in individual sections than in these composite sections (see section 3.2.3).

In contrast, the third population of partially mixed water between the EDDY and offshore water (Fig. 5) is all found poleward of the EDDY region (Fig. 6a, b) as water with a weaker spice anomaly ( $\gamma \approx 0.1 \text{ kg m}^{-3}$ , pink colors). This water is not as warm as offshore water, indicating some mixing with offshore water has taken place. Of note is that this intermediate water mass appears completely absent in the sections further equatorward

(Fig. 6c, d), indicating that it is either mixed away or that it is advected elsewhere; we argue below that it is advected offshore in a large-scale tongue.

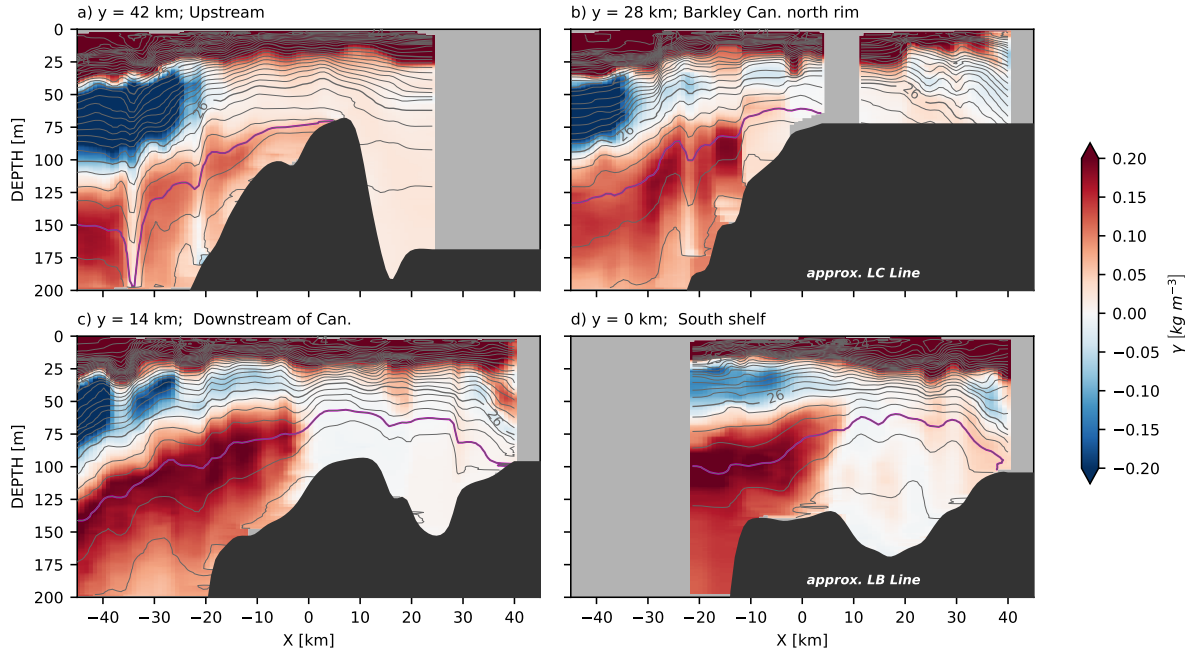


**Figure 6.** Synthetic sections of spice anomaly from the MVP data, projected along four lines from poleward (upstream of coastal current) a) to equatorward (downstream); the lines are shown in Fig. 1b<sup>a</sup>). Isopycnals are contoured every  $\sigma_\theta = 0.2 \text{ kg m}^{-3}$ , with the  $\sigma_\theta = 26.4 \text{ kg m}^{-3}$  isopycnal highlighted in magenta. Colors are spice anomaly as defined in Fig. 5. "BC" in panel (c) refers to Barkley Canyon. Note that b) is along LC line (Fig. 3a–c,g–i), and d) is along the LB line (Fig. 3d–f,j–l).

Oxygen saturation sections show that the deep water in the EDDY has very low oxygen saturation (Fig. 7c, d) compared to surrounding water (though again, we caution against the quality of these saturation values from such a fast profiling instrument with a slow response time). More oxygenated water is found offshore, and the oxygen deficit is not as strong in the poleward sections (Fig. 7a, b). The T/S compensated front also shows an abrupt transition from the EDDY water and the offshore. Note the excellent correlation between oxygen saturation and spice anomaly in Fig. 6.

The spatial patterns are very clear when considering a map view of properties along the  $\sigma_\theta = 26.4 \text{ kg m}^{-3}$  isopycnal (Fig. 8). There is a region onshore of the south tip of La Perouse Bank (approximately 44.5°N, 125.75°W), that consists of water that is found along the mixing line (spice anomaly  $\gamma \approx 0 \text{ kg m}^{-3}$ ) that also has low oxygen saturation. Offshore of this region is water that is very warm and salty in comparison ( $\gamma > 0.15 \text{ kg m}^{-3}$ ), and relatively high in oxygen (saturation of approximately 60%). The region transition between these two water masses is very abrupt, and stretches from La Perouse Bank to a shallow bank just above the Juan de Fuca canyon (48.3°N and 125.4°W).

Poleward of La Perouse bank and Barkley Canyon, the water along the shelf has the weaker spice anomaly characteristic of the third water mass ( $\gamma \approx 0.1 \text{ kg m}^{-3}$ , light pink colors). This water is also somewhat lower in oxygen than water from offshore, though not as depleted as the water in the EDDY. This water appears to be pushed offshore just

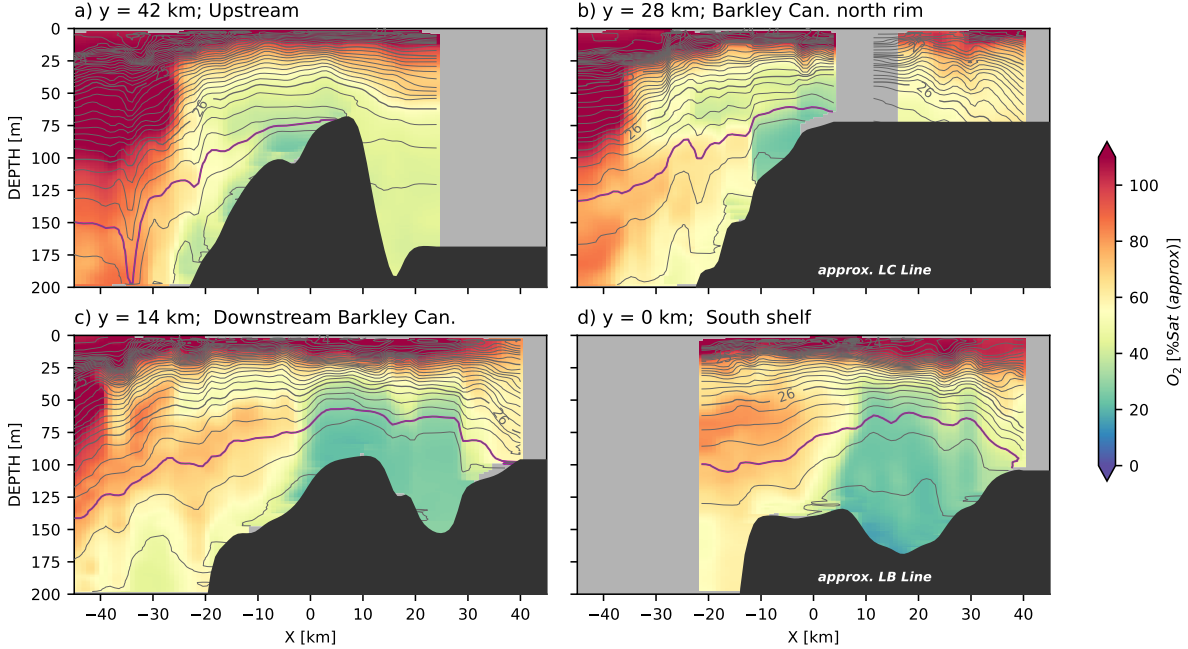


**Figure 7.** As in Fig. 6, for oxygen approximate saturation.

upstream of Barkley Canyon and replaced on the shelf by the warmer (high spice) offshore water.

The correspondence between low oxygen water and water on the mixing line that defines  $\gamma \approx 0 \text{ kg m}^{-3}$  is quite strong (Fig. 8c). Eddy water is onshore (more red colors), low in oxygen, and along the mixing line. Offshore water is high in oxygen and has a high spice anomaly. Water that is found poleward on the shelf is still relatively high oxygen, but of intermediate spice  $\gamma \approx 0.125 \text{ kg m}^{-3}$ .

### 3.2.2 Spur Canyon

The Spur Canyon leading from the Strait of Juan de Fuca has been implicated in allowing dense water to be upwelled into the EDDY (Mackas et al., 1987; Weaver & Hsieh, 1987). The sea surface is low in the middle of the EDDY, so it has been hypothesized that water moves up the Spur Canyon due to ageostrophic motion (Weaver & Hsieh, 1987; Freeland & Denman, 1982). This It is difficult to infer flow up the Spur Canyon from the observations collected here. Three transects up the canyon indicate that deep isopycnals slope up into the canyon (Fig. 9, to approximately 30 km). Continuing across the EDDY, isopycnals are largely flat until they intersect the Vancouver Island Coastal Current ( $80 \text{ km} X_{\text{canyon}} = 80 \text{ km}$ ). The deeper isopycnals are not found in the deeper basin northeast of La Perouse bank Bank (70 km), thus the bank is a natural poleward boundary of the EDDY.

Spice anomaly along the canyon indicates a transition from offshore water to EDDY water. Oxygen saturation behaves in a similar manner, though some of the incoming water has slightly lower oxygen than water inside the EDDY (not shown). Based on these sections, it is difficult to infer water motion up the canyon.

Much of the modified water in the Spur Canyon appears to come from the shelf to the west, but heavily modified by tidal mixing. A repeat tidal survey over the bank on the west side of the canyon shows a strong hydraulic response during onshore flow (17:58–21:00,

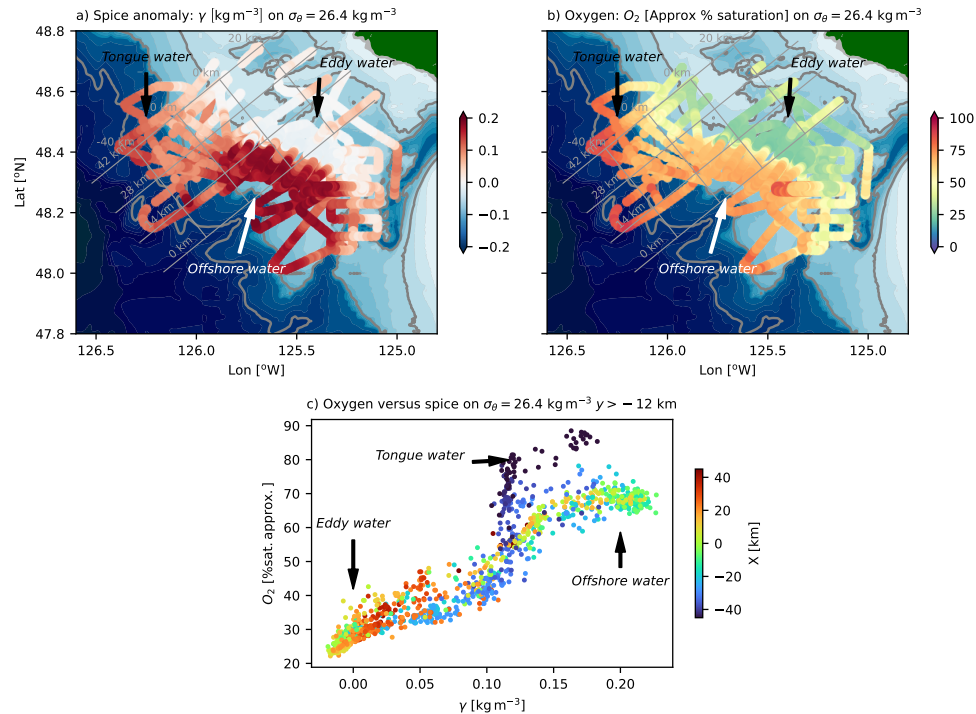


**Figure 8.** Spatial overview of a) the spice anomaly, and b) oxygen saturation on the  $\sigma_\theta = 26.4 \text{ kg m}^{-3}$  isopycnal. Grey cross-slope lines are cross sections indicated in Fig. 6. Along-slope grey lines are every 20 km in the cross-slope direction, with  $X = 0 \text{ km}$  near the 100-m isobath at the north end of the observation area. c) distribution of oxygen as a function of spice anomaly and  $\sigma_\theta = 26.4 \text{ kg m}^{-3}$ , colored by x-coordinate. Data from the Juan de Fuca Canyon region ( $y < -12 \text{ km}$ ) is not shown.

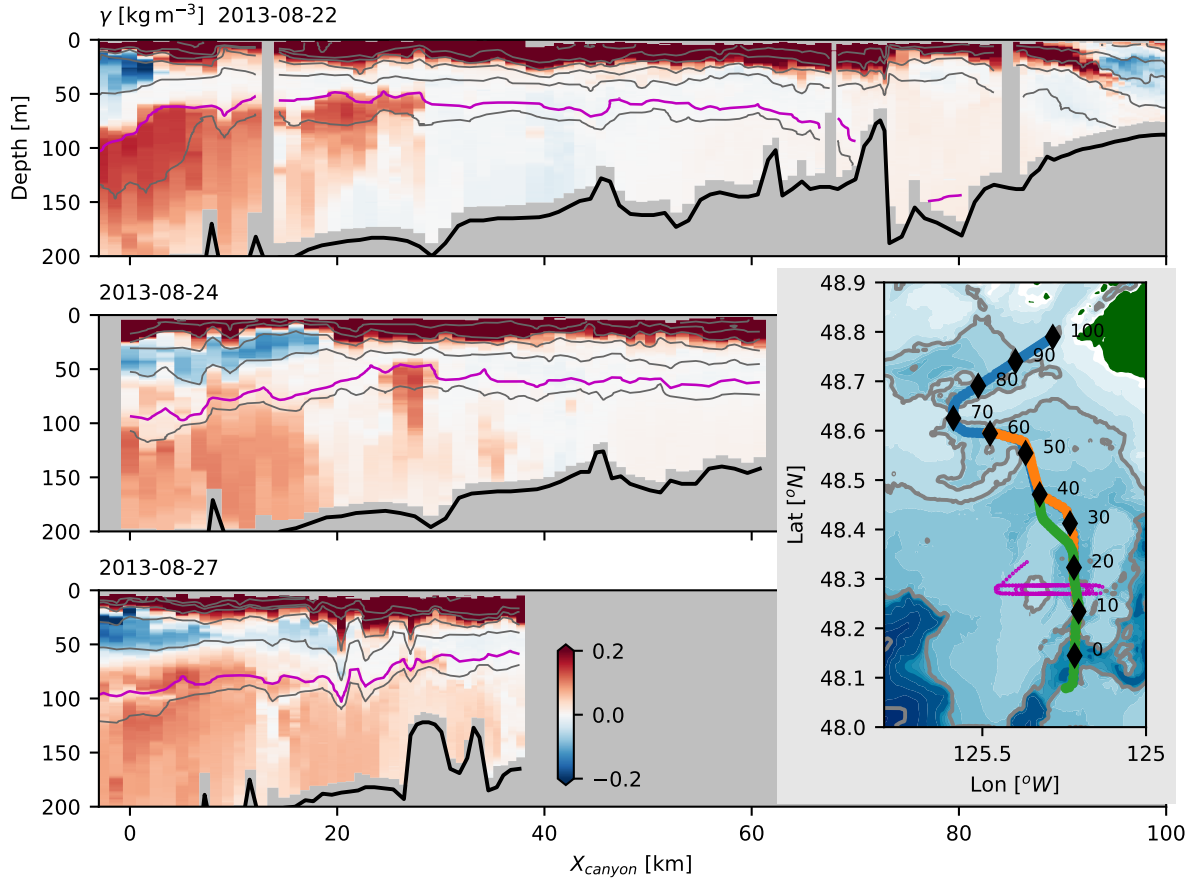


**Figure 9.** Spice anomaly surveys up the Spur Canyon, where  $\underline{X-X}_{\text{canyon}}$  is along-canyon as defined in the map. Grey isopycnals are contoured every  $0.5 \text{ kg m}^{-3}$ , and the  $26.4 \text{ kg m}^{-3}$  isopycnal is shown in magenta. The seafloor is indicated with the thick black line. Map (lower right) shows the path taken during each survey in chronological order (blue, orange, and green). Magenta line is path taken during a cross-canyon survey (Fig. 10).

284 Fig. 10). Dense water passes from the offshore side into the canyon, and plunges down  
 285 the side wall before rebounding downstream. Note that the tide here is largely diurnal, so  
 286 this onslope flow only occurs once a day. Given the stratification of  $N \approx 6 \times 10^{-3} \text{ rad s}^{-1}$   
 287 and an overturning scale of 50 m, we might expect dissipation rates reaching  $\epsilon \sim L^2 N^3 \approx$   
 288  $5 \times 10^{-4} \text{ m}^2 \text{s}^{-3}$ , which is three orders of magnitude higher than dissipation observed on  
 289 the shelf west of this location by Dewey and Crawford (1988). This estimate of turbulence  
 290 dissipation rate implies a diapycnal diffusivity of  $\kappa = \gamma \epsilon / N^2 \approx 1 \text{ m}^2 \text{s}^{-1}$   $\kappa = \gamma \epsilon / N^2 \approx 0.5 -$   
 291  $5 \text{ m}^2 \text{s}^{-1}$ , assuming a mixing efficiency of  $\gamma = 0.2$ . Water spills over from the offshore front  
 292 into the canyon during the onshore tide. This water is rapidly mixed with surrounding water  
 293 such that its strong offshore spice values are attenuated.

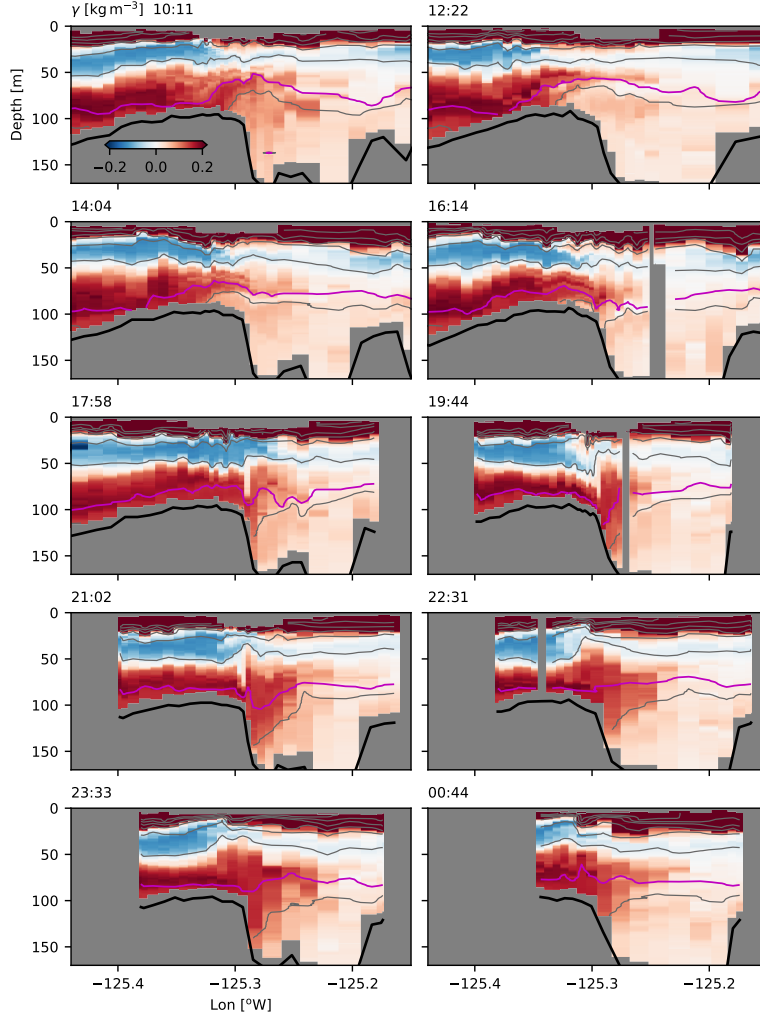


**Figure 10.** Spice anomaly observed in repeated, tide-resolving survey across the Spur Canyon, time is indicated in the upper left of each plot (29 August, 2013). Location of survey shown in Fig. 9 as a magenta line.

294 The turbulence found on the canyon rim makes it ambiguous if there is water moving  
 295 up the canyon or not. There is a general tendency along the canyon for higher spice water  
 296 to be found offshore (Fig. 9) but it seems likely that the source of the higher spice water  
 297 is from over the bank rather than water being advected up the canyon. ~~This~~ ~~The~~ tidally

298 driven flow over the bank is the most significant source of high-spice offshore water into the  
 299 ~~eddy~~EDDY region identified during our surveys.

### 300 3.2.3 *Frontal survey*

301 A systematic survey through the front between the offshore water and the EDDY water  
 302 demonstrates the sharpness and persistence of this front (Fig. 11), suggesting that it has  
 303 limited exchange with the offshore region.

304 The survey started close to shore, and passed through the Vancouver Island Coastal  
 305 Current (along-track 0-10 km). The coastal current forms a buoyant ~~front~~current, and is  
 306 fresher and colder than water at the same density. ~~This front~~The front with the coastal  
 307 water is relatively thick, greater than 20 km wide, and has entrained partially mixed water  
 308 down from the surface to the foot of the front ( $\gamma \approx 0.1$ ).

309 Offshore of this coastal current, measurements were collected crossing the front be-  
 310 tween the offshore water and the EDDY water 10 times, showing its evolution following the  
 311 along-shore equatorward flow. First, as noted in the composite sections, isopycnals slope  
 312 up from offshore onto the shelf. In the first crossing, the front is very sharp, (along-track  
 313 distance 50 km) though two small tendrils of higher spice water can be seen separating from  
 314 the front on the inshore side. Similar tendrils are found on the second crossing, perhaps a  
 315 bit more separated from the front ( $\approx 80$  km), and on the third crossing ( $\approx 95$  km). These  
 316 tendrils are made of up partially mixed water. The subsequent passes have more of this  
 317 partially mixed water, such that the partially mixed front is up to 5-km wide by the fifth  
 318 pass ( $\approx 150$  km). However, the deeper isopycnals retain a sharp front, and indeed the front  
 319 appears sharp again by the seventh pass at all depths ( $\approx 200$  km).

320 There is evidence of some warmer water swirling into ~~Eddy~~EDDY, particularly along  
 321 isopycnals deeper than  $26.4 \text{ kg m}^{-3}$ . Regions of warmer (and more oxygenated) water are  
 322 found in tendrils at these depths (e.g.  $\approx 170$  km  $\approx 170$  km and  $\approx 185$  km). The overall  
 323 effect is similar to what was seen in the Gulf Stream with similar observations (Klymak et  
 324 al., 2016); there are two quite distinct water masses, the ~~Eddy~~EDDY water and the offshore  
 325 water, as seen in the  $\theta$ - $S$  plot (Fig. 11c) with only a small population of samples between  
 326 these two. ~~This distribution of~~These distinct  $\theta$ - $S$  properties ~~is~~are indicative of substantial  
 327 isopycnal and vertical mixing, but even these populations are relatively cut off from the main  
 328 water masses, indicating that they are well-mixed on their own, in short episodic events.  
 329 Regardless, this front is very sharp given that it has no density signature, indicating that  
 330 there is not strong advection from offshore into the EDDY region.

### 331 3.3 Separation of coastal water

332 Upstream of the the sharp front between the low-spice EDDY and the high-spice off-  
 333 shore water is a substantial mass of intermediate-spice water along the shelf (compare Fig. 6a  
 334 and c). This intermediate spice water is moving equatorward along the shelf upstream of  
 335 the EDDY, but is pushed offshore just upstream of Barkley Canyon (Fig. 12d). There is a  
 336 tongue of intermediate-spice water ( $\gamma$  ~~is~~ $\approx 0.1 \text{ kg m}^{-3}$  pink along  $26.4 \text{ kg m}^{-3}$ ) that sep-  
 337 arates from the shelf just west of  $126^\circ\text{W}$ . The surveys do not cross the full extent of the  
 338 tongue, but it is at least 30 km wide. It also appears to end at approximately  $48.2^\circ\text{N}$ . This  
 339 intermediate-spice water reaches from relatively shallow isopycnals to at least  $26.6 \text{ kg m}^{-3}$   
 340  $26.55 \text{ kg m}^{-3}$  (Fig. 12, left panel h). Unfortunately, we cannot track the fate of this wa-  
 341 ter mass because isopycnals tilt down offshore, below the depth limit of the MVP. The  
 342  $25.5 \text{ kg m}^{-3}$   $25.8 \text{ kg m}^{-3}$  isopycnal appears to have the tongue (Fig. 12a), but closer to the  
 343 shelf than at  $26.4 \text{ kg m}^{-3}$ , indicating strong three-dimensionality to this feature.

344 This separating tongue is embedded in the larger scale isopycnal tilt caused by the  
 345 upwelling (Fig. 12, right panels c, f, and j), so it is difficult to see dynamically what is driving  
 346 this offshore push. If the offshore motion were geostrophically balanced, we would expect the

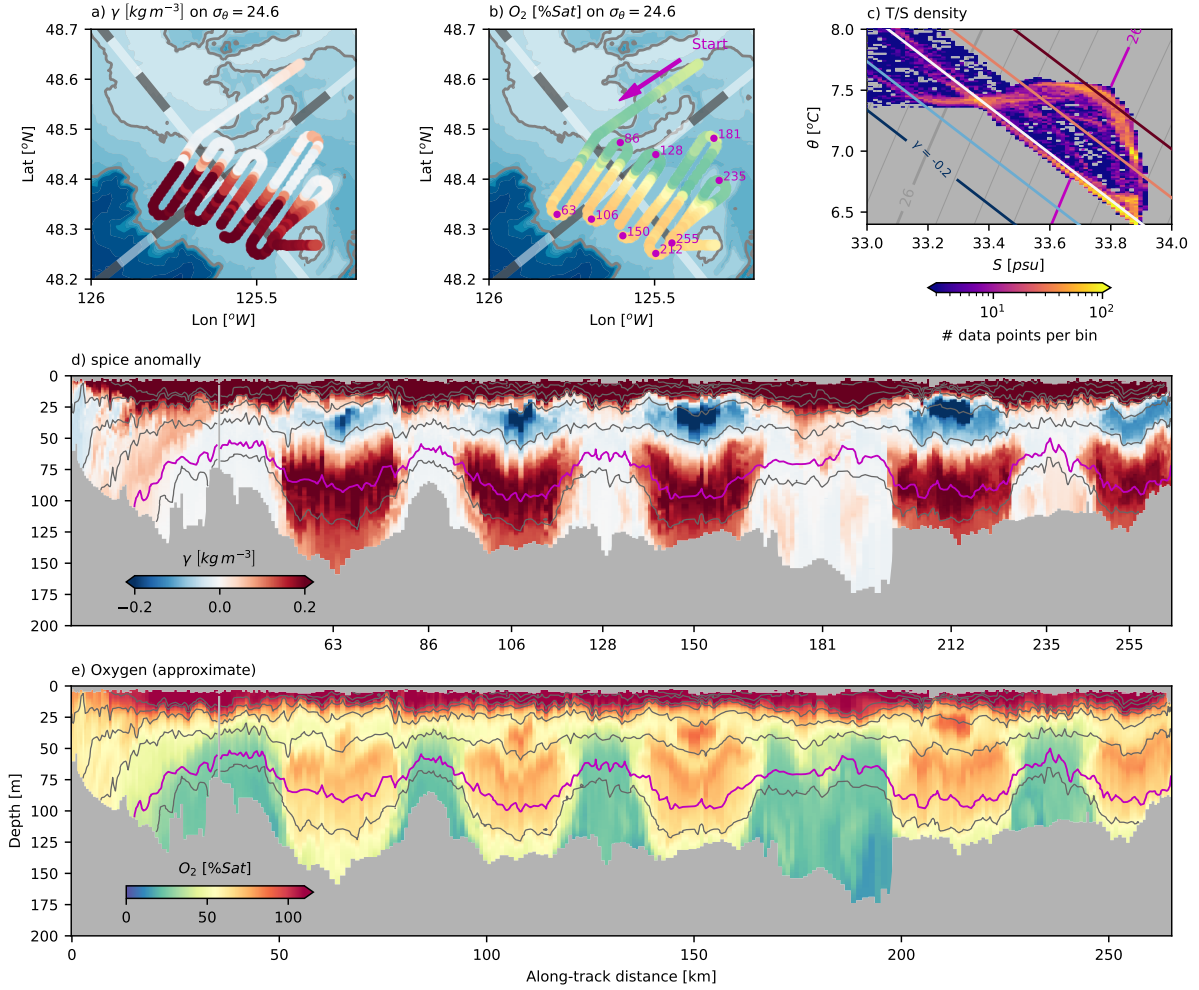


**Figure 11.** Data from the [frontal-offshore front](#) survey a) spice anomaly along  $26.4 \text{ kg m}^{-3}$ . Grey-white alternating lines are the coordinate system, with 10-km alternating shades. b) oxygen saturation along  $26.4 \text{ kg m}^{-3}$ ; magenta dots correspond to [turn locations as](#) distance along-track. c) density of data points (logscale) in this section of data. d) cross-section of spice anomaly along track. Grey isopycnals are contoured every  $0.5 \text{ kg m}^{-3}$ , and the  $26.4 \text{ kg m}^{-3}$  isopycnal is shown in magenta. [Ticks are turn locations](#) e) cross-section of oxygen saturation.

347 isopycnals to dome upwards from poleward towards Barkley Canyon, but if such doming is  
 348 happening, it is weaker than variability from internal tides and synoptic unsteadiness. One  
 349 possibility is that it is simple flow separation caused by the water not being able to make  
 350 the sharp turn around La Perouse Bank, which would be an ageostrophic effect. Whatever  
 351 causes it, downstream of the separation, the water is replaced by offshore water with much  
 352 higher spice values. The high-spice water comes onto the shelf through much of the water  
 353 column, so is not just being carried onshelf by near-bottom Ekman layer by wind driven  
 354 upwelling.

355 There is a clear surface expression of the separating tongue in satellite imagery (Fig. 13).  
 356 Water flowing equatorward along the shelf tends to be cooler than offshore water, likely due  
 357 to mixing with the colder coming out of the Strait of Juan de Fuca. On August 25, there is a  
 358 cold tongue of water separating from La Perouse bankBank, crossing isobaths and pointing  
 359 south at 125.8°W. There is a cooler tendril streaming west at 48 N off the south end of  
 360 this tongue. This feature is not as well-developed in the previous image (Aug. 21) perhaps  
 361 indicating that it is an evolving feature. By 31 August, there is no surface expression of  
 362 the feature, though small tendrils of cooler water can be seen separating from La Perouse  
 363 Bank. By 5 September, the water has significantly warmed, and the offshore anomaly does  
 364 not appear to have a surface signature.

365 Satellite-based surface chlorophyll estimates show the same feature (Fig. 14) demonstrating  
 366 suggesting the advection of high chlorophyll to the west side of the EDDY. They also show  
 367 a relatively high-chlorophyll tendril to the west, again exiting the study region at approxi-  
 368 mately 48 degrees N. The feature is relatively long-lived, on the order of one month. Inspec-  
 369 tion of images before August 5 were too obscured by clouds or did not show this feature.  
 370 By September 6, we see the feature fading from the satellite image. Note that this feature is  
 371 centered 0.2 degrees of latitude south of tongue that we observe deeper in the water column,  
 372 again indicating that there is depth-dependent structure in the feature.

## 373 4 Summary and Discussion

374 The intensive sampling discussed here has demonstrated a few important features of  
 375 the South Vancouver Island Shelf. The Juan de Fuca Eddy water is readily identified as  
 376 falling along a mixing line in  $\theta$ - $S$  space, compared with offshore water that was warmer and  
 377 saltier (high-spice anomaly). There was not strong evidence of the EDDY being supplied by  
 378 water moving up the Spur Canyon during our observations, but the Spur Canyon was a site  
 379 of hydraulic cross-canyon flows in which we infer significant mixing has occurred. There is a  
 380 sharp and persistent temperature-salinity compensated front between offshore water and the  
 381 partially mixed EDDY water. Finally, upstream of the EDDY, water in the equatorward shelf  
 382 current has intermediate spice anomaly, and is seen to separate from the shelf at the point  
 383 of an abrupt bend in an underwater bank. The water mass crosses isobaths and is ejected  
 384 into the interior. This separation event can also be observed from satellite measurements  
 385 of sea surface temperature and chlorophyll. Thus the water that is offshore of the EDDY  
 386 appears to have been brought onto the shelf in exchange for the offshore ejection of shelf  
 387 water via this tongue.

### 388 4.1 Age and source of the EDDY water

389 The source of water and formation mechanism of the Juan de Fuca Eddy has received  
 390 substantial attention, however, the observations of EDDY waters being found along a tight  
 391 mixing line in  $\theta$ - $S$  space has not previously been noted. The deepest water in the EDDY  
 392 could originate along the  $\theta$ - $S$  line from approximately 5.5°C to 7.5°C (Fig. 4a), which in  
 393 the open ocean spans depths from 420 m to 70 m. Mackas et al. (1987) attempted to  
 394 determine the origin of the water by including oxygen as a third variable to resolve the  
 395 ambiguous  $\theta$ - $S$  relation. However, as Fig. 4b makes clear, oxygen does not appear to be  
 396 a conserved property in the EDDY, with concentrations up to 150  $\mu\text{mol kg}^{-1}$  lower in the

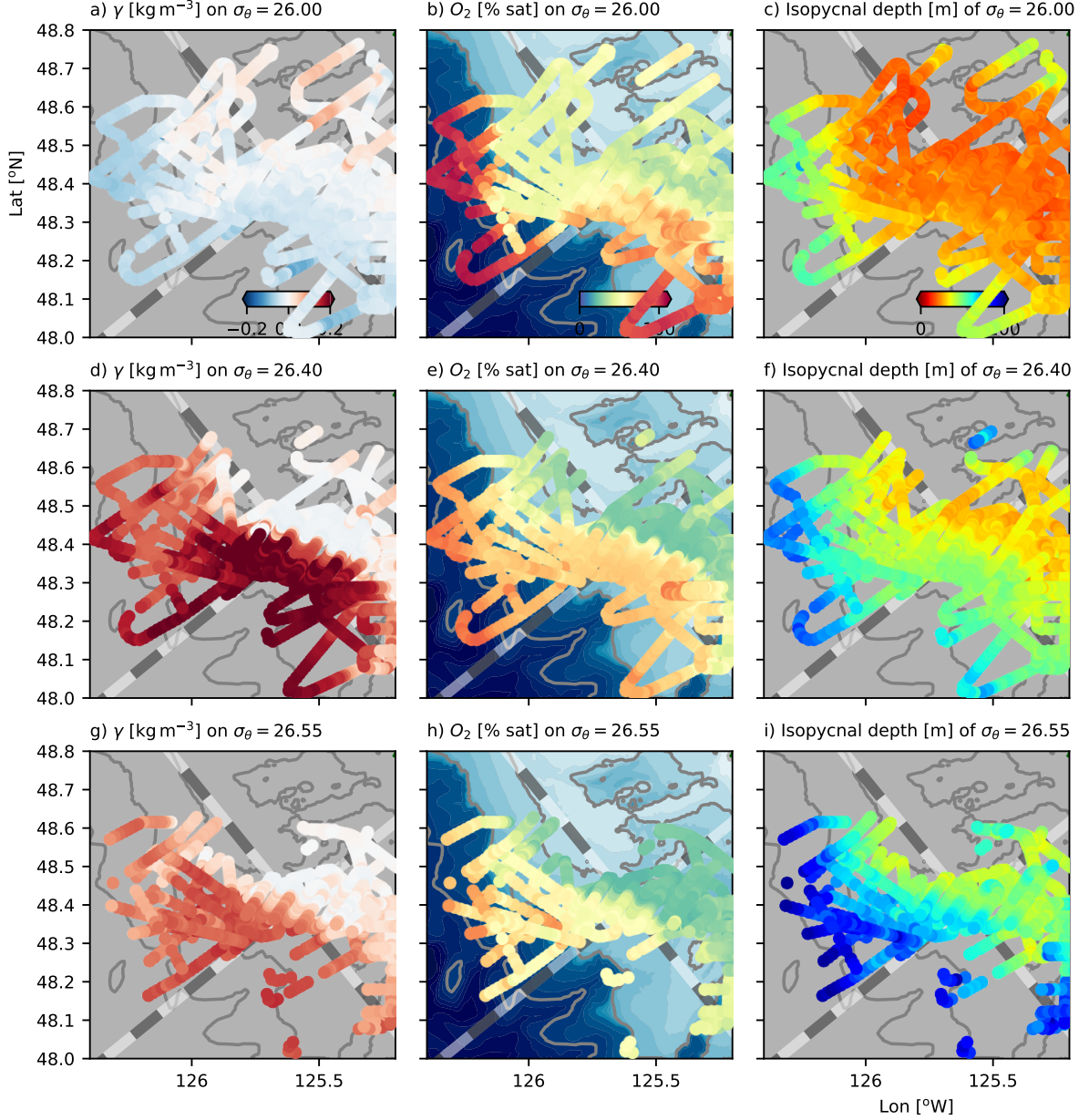


**Figure 12.** Isopycnal slices [through-of the MVP data](#) showing the vertical structure of the water separating from the shelf, with the first row along  $25.5 \text{ kg m}^{-3}$ , second along  $26.4 \text{ kg m}^{-3}$ , and the third at  $26.6 \text{ kg m}^{-3}$ . First column is the spice anomaly, second is oxygen saturation, and the last column is depth of each isopycnal.

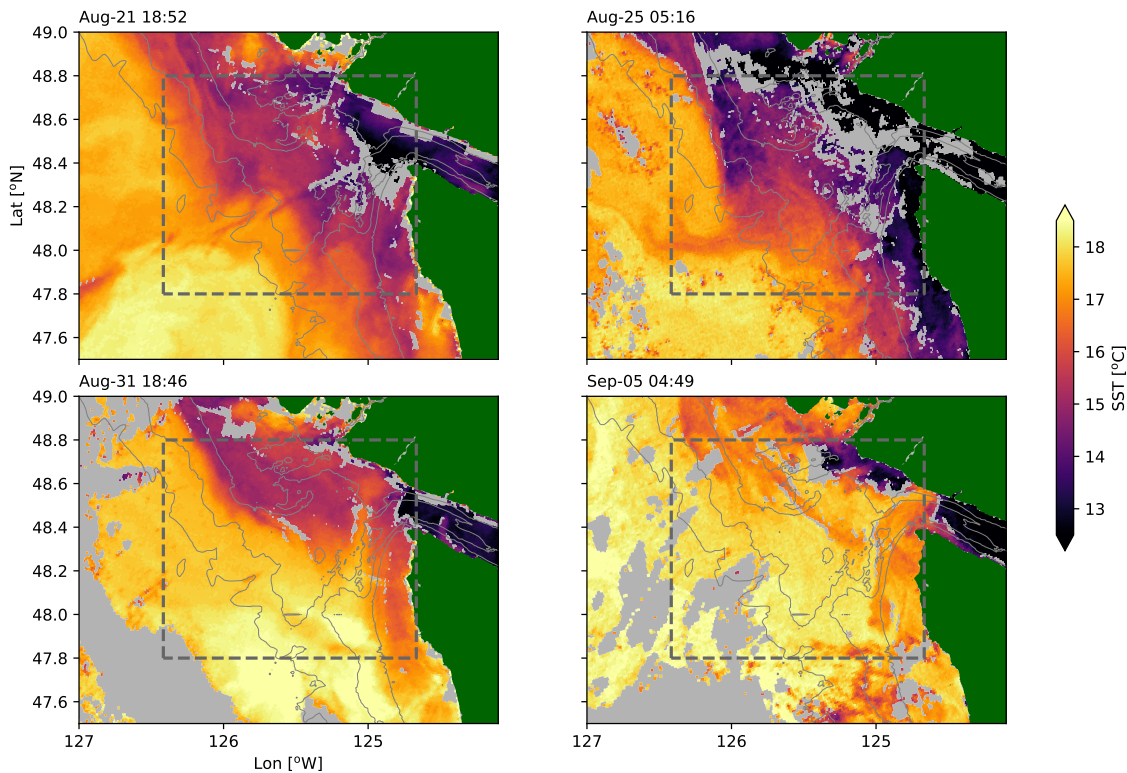


**Figure 13.** Sea surface temperature snapshots from the observation period. Grey areas are clouds; dashed gray line is the study area. Depths are contoured in thin gray lines at 200, 150 and 100 m. (OSI SAF, 2015)

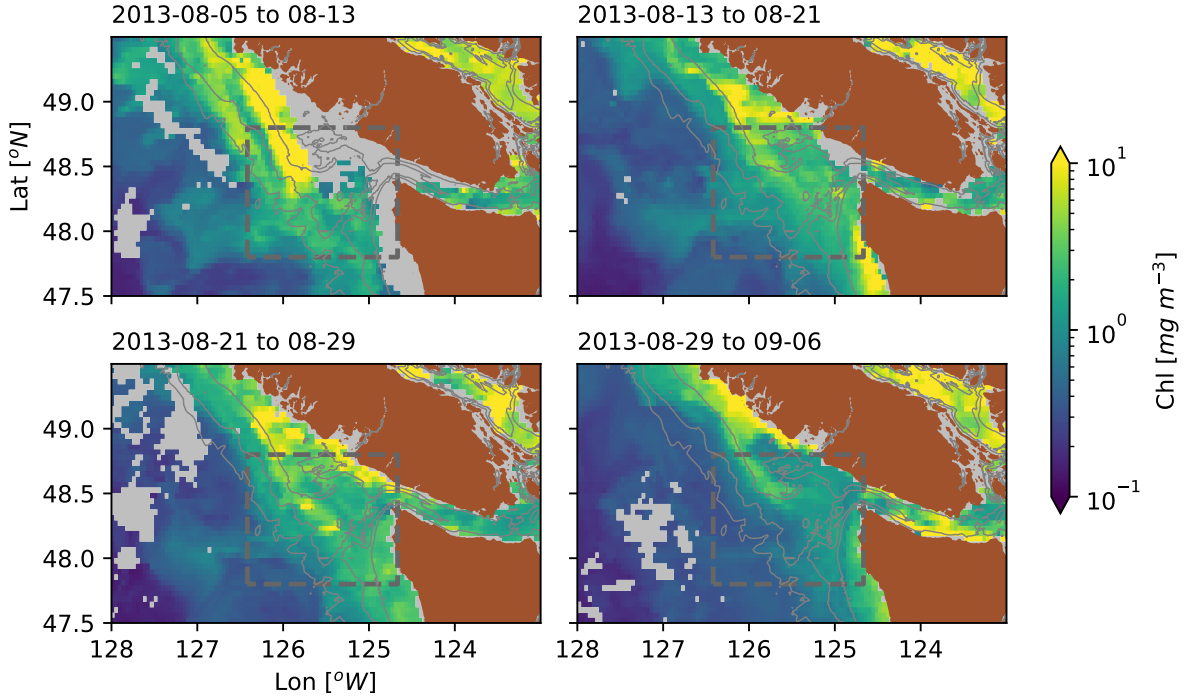


**Figure 14.** Surface chlorophyll density estimated from ocean color (Hu et al., 2012; NASA Ocean Biology Processing Group, 2017) over 8-day windows in 4-km bins. Gray regions had too many clouds to compute averages.

EDDY than the water found offshore, and in a way that definitely cannot be the result of conservative mixing. As a best guess, if the water in the deepest part of the EDDY came from a vertical mixture of the water at  $26.5 \text{ kg m}^{-3}$  and an equal distance down in density space of  $26.7 \text{ kg m}^{-3}$ , then the deepest water in the EDDY may be coming from a depth of 250 m. This is a typical upwelling depth for coastal flows, and may not require extra input up the Spur Canyon as posited by Freeland and Denman (1982).

We found little evidence of flow up the Spur Canyon or, if there is, then the mixing in the canyon is intense enough to remove the  $\theta$ - $S$  signature of offshore water within 20 km of the canyon mouth (Fig. 9). We did find substantial evidence of mixing in the canyon, but the primary pathway of high-salinity water into the canyon appears to be due to tidal flow over the banks on the west side (Fig. 10), rather than flow up the canyon. However, it is worthy of note that upwelling winds had ceased at the point of these observations (Fig. 2), so the offshore surface pressure gradient may be reduced, leading to reduced ageostrophic upwelling in the canyon. Whether the cessation of winds would also lead to a reduction of the low sea level height in the center of the EDDY that may drive up-canyon flow is an open question.

There is evidence of aging of the water in the EDDY between late spring and late summer (Fig. 3), with a reduction of oxygen in the EDDY over this time span. If we posited that the reduction was all in the same water, then the oxygen consumption rate over the time between the late-May and early September cruises would be on the order of  $0.5 \mu\text{mol kg}^{-1}\text{d}^{-1}$ . This is on the low side of estimates of apparent oxygen utilization rates in continental upwelling systems, which are between 1 and  $5 \mu\text{mol kg}^{-1}\text{d}^{-1}$  (Dortch et al., 1994) (Dortch et al., 1994; Connolly et al., 2010). So it seems ~~possible~~ likely that the EDDY ~~had enough~~ has exchange with the surrounding water ~~for the residence time~~

421 ~~to have been less than the full time period from late May to September.~~ Note that during  
 422 the May cruise, the water in the EDDY is slightly cooler than the mixing line, and during  
 423 the September cruise is slightly warmer than the mixing line, ~~so further evidence that~~ the  
 424 water in the EDDY is evolving seasonally, ~~and probably affected by the water temperature~~  
 425 ~~in the~~ (Fig. 3e,k). This is consistent with findings on the Oregon shelf where physical  
 426 processes are thought to account for 55–70% of changes in dissolved oxygen concentrations  
 427 (Adams et al., 2013). Definitively identifying the exchange mechanisms into the EDDY is  
 428 challenging from this data set. The offshore front does not appear to have much exchange,  
 429 however as noted above there does appear to be strong tidal flows and mixing over the  
 430 submarine banks that can transport more oxygenated water into the EDDY. Further, the  
 431 Vancouver Island Coastal Current ~~and the amount of water getting through the onshore~~  
 432 ~~front is oxygen-rich and has a much less sharp front than the offshore front~~ (Fig. 11), and is  
 433 a likely source of oxygen to the EDDY.

434 The water is mixed enough in the EDDY that it falls along a mixing line, though it  
 435 remains vertically stratified. The amount of homogenization is such that either the mixing is  
 436 very strong, or the water is retained in the EDDY for a long time. The amount of turbulence  
 437 required to homogenize 100 m of water over 90 days is  $\kappa \approx 10^{-3} \text{ m}^2 \text{s}^{-1}$ . Given that the diffu-  
 438 sivity implied in the cross-channel surveys was on the order of  $\kappa_p = 10 \text{ m}^2 \text{s}^{-1}$ ,  $\kappa_o = 0.5-5 \text{ m}^2 \text{s}^{-1}$ ,  
 439 this number is not outrageous if we think that such high dissipation is found in ~~10<sup>-4</sup>~~  
 440 ~~0.2–0.02%~~ of the water column. We can more carefully quantify this by considering a  
 441 synthetic profile of temperature and salinity based on an offshore profile, extrapolated from  
 442 the bottom of the 200-m cast to 250 m, assuming that the temperature and salinity at 250  
 443 m are 6.2 [°C] and 34 psu respectively (Fig. 15). Water at the offshore station was warmer  
 444 than onshore, so the profile was also linearly interpolated to a surface value of (12 °C,  
 445 31.6 psu). The profile was then linearly compressed into a depth range of 150 m representa-  
 446 tive of the shelf depth in the dense pool, and subjected to mixing with a constant diffusivity  
 447 of  $\kappa = 10^{-3} \text{ m}^2 \text{s}^{-1}$ , with the surface and bottom values pinned under the assumption that  
 448 the near-bottom source and surface waters are replenished from a large reservoir. ~~Similar to~~  
 449 ~~the naive scaling in this calculation~~, the T-S relationship does not approach a straight line  
 450 until after approximately 60–100 days, or until the mixing affects a vertical length scale of  
 451  ~~$\lambda = (\tau\kappa)^{1/2}$  that is greater than  $\approx 70 \text{ m}$~~   $\lambda = (\tau\kappa)^{1/2} \geq 70 \text{ m}$ .

452 Combined with the oxygen observations, the implication is that the water in the EDDY  
 453 likely experiences exchange with the outside water, but at a very modest rate. In terms of a  
 454 volume flux, we might estimate the EDDY area as  $900 \text{ km}^2$ , over 100 m depth, so that 100-d  
 455 residence time corresponds to a transport of  $10^4 \text{ m}^3 \text{s}^{-1}$ , which is remarkably weak for the  
 456 transport in and out of such a large area.

457 The sharpness of the front with the EDDY and the offshore water is intriguing. It was  
 458 persistent for the duration of our detailed survey (Fig. 8), and, so far as we can tell with  
 459 the limited resolution of the hydrographic surveys, was present during the bracketing La  
 460 Perouse cruises. There is not any substantial bathymetry blocking the onshore incursion of  
 461 water at this location, so there must be a dynamic barrier.

462 Numerical simulations of this region reported by (Sahu et al., 2022) using a NEMO  
 463 36th-degree regional model contained relatively rapid exchange between the deep EDDY  
 464 water and the rest of the coastal ocean. The region where the EDDY resides has velocities  
 465 equal or greater than other parts of the shelf, and water has an approximate residence time  
 466 of less than 20 days. The EDDY water in the model does develop a distinct  $\theta$ -S signature,  
 467 but not along a sharp mixing line as observed. It also has a front with the offshore water,  
 468 but the front is substantially wider than that observed here. ~~Overall it seems that the~~  
 469 ~~model sees stronger cross-shelf advection than are apparent in these observations, though~~  
 470 ~~the reason for this will require further study.~~

471 Overall, it would be an improvement to our understanding of the EDDY if we could  
 472 sample the shelf more persistently. The EDDY was already well-formed by the May La

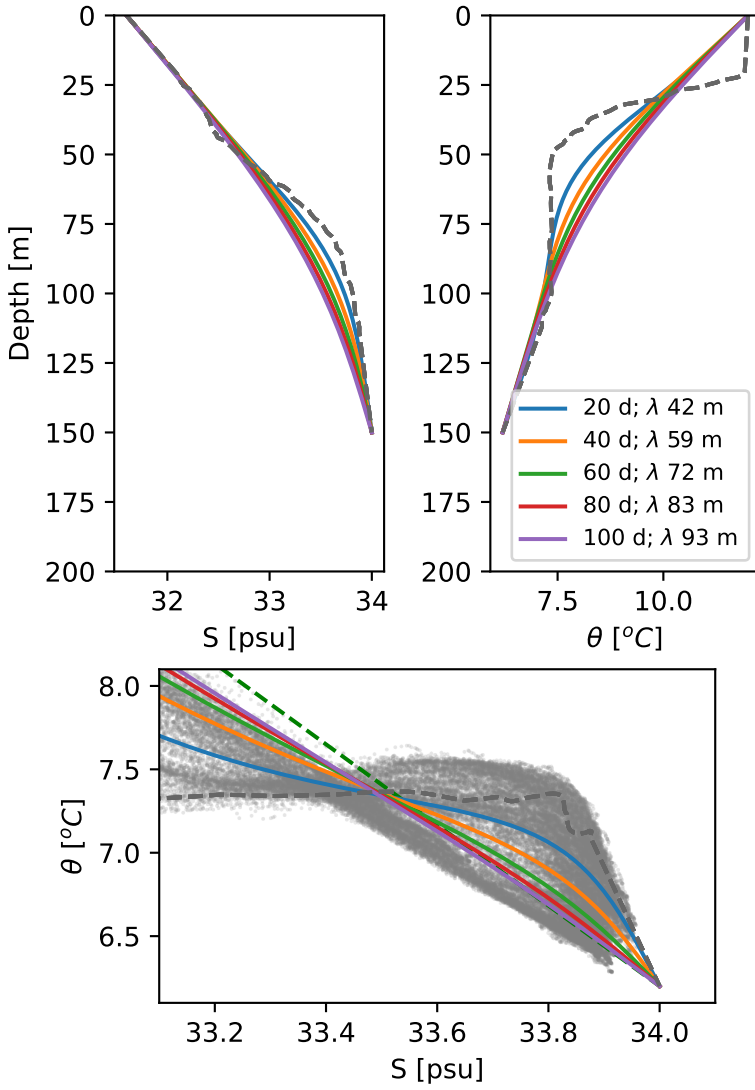


**Figure 15.** Mixing model assuming constant eddy diffusivity of  $\kappa = 10^{-3} \text{ m}^2 \text{s}^{-1}$  acting on an offshore temperature and salinity profiles compressed from 250 thick to 150 m thick (grey dashed lines). Profiles are pinned to the deep  $\theta - S$  value at (34 psu, 6.2 °C), and a shallow one at (31.6 psu, 12 °C). The green dashed line is the mixing line defined in the text.

473 Perouse cruise, and seems to evolve slowly during that time. Capturing its formation,  
 474 presumably earlier in the spring, as well as its evolution through the year, would be valuable  
 475 in understanding retention and exchange on this productive part of the shelf.

#### 476 4.2 Offshore exchange of shelf water

477 The displacement of shelf water from La Perouse Bank is a dramatic departure from  
 478 geostrophically balanced isobath-following flow. Eddies have been known to separate from  
 479 irregular coastal topography, both at the surface (Barth et al., 2000) and deeper in the  
 480 water column (Pelland et al., 2013). It has been recognized that instabilities lead to exchange  
 481 between the open ocean and the shelf at this location (Ikeda & Emery, 1984, 1984). However,  
 482 observations of the wholesale replacement of shelf water by a new water mass from offshore  
 483 are relatively rare. In the observations presented here, it is clear that water from as deep as  
 484 150 m is separating from the shelf and moving offshore (Fig. 8, Fig. 12).

485 Satellite imagery shows that there is often exchange between coastal and deep waters  
 486 along the Vancouver Island shelf (Fig. 16). Most years there are three of four large filaments  
 487 from the shelf into the open ocean, many of them over 100 km long. This length scale is  
 488 longer than the 60 km inferred for this region by Ikeda et al. (1984) using a four-layer  
 489 instability analysis. It is possible that there is spatial locking of these features, with a  
 490 persistent separation at the north tip of Vancouver Island, and a strong tendency for one  
 491 at 49.5 N. There is also evidence of separation events in most of the years, with 2011  
 492 being the only clear exception. General baroclinic instability of the upwelling front is a  
 493 possible mechanism to drive offshore exchange (Ikeda et al., 1984; Durski & Allen, 2005),  
 494 but this tends to be shallow, with smaller-scale instabilities that will not extend as far into  
 495 the interior ocean as observed here. Rather it seems likely that the topographic change  
 496 engendered by the sudden turn to the east of La Perouse ~~bank~~Bank catalyses a larger scale  
 497 instability at this location. In California most of the cold filaments observed appear to be  
 498 catalyzed by headlands and underwater topography (Strub et al., 1991), though modelling  
 499 studies find instabilities are possible even in two-dimensional flows (Pierce et al., 1991).  
 500 Durski and Allen (2005), when modelling the Oregon shelf, found that including realistic  
 501 shelf bathymetry catalyzed intermittent large-scale instabilitiessimilar to the feature here,  
 502 a finding that is deemed likely to apply at other coastal locations (Battieen, 1997).

503 Large-scale mixing between the shelf and open ocean has been evident since the satellite  
 504 era. Here we demonstrate that in the Vancouver Island shelf the flow is originating on the  
 505 shelf and separating from the bathymetry and being injected into the interior. A similar  
 506 observation was made by Barth et al. (2000) downstream of Cape Blanco, Oregon, where  
 507 the coastal current was observed to detach from the shelf in the lee of the cape and flow into  
 508 the interior. They hypothesized that as the current moved offshore, it deepened, stretching  
 509 isopycnals and creating cyclonic relative vorticity that would tend to push the current back  
 510 onshelf, but then it was caught in the undercurrent and stalled, being pushed offshore. It is  
 511 also possible that coastally trapped waves in the region experience a hydraulic control, and  
 512 these separation events are part of the response (Dale & Barth, 2001).

513 Regardless of the dynamics of the separation events, the offshore transport can be  
 514 substantial. If we assume the coastal current is approximately  $0.1 \text{ m s}^{-1}$  over 100 m in  
 515 the vertical and 20 km in the horizontal, it represents 0.2 Sv of nutrient- and chlorophyll-  
 516 rich shelf water transported offshore. Sometimes the along-shelf currents are substantially  
 517 larger than this (Thomson & Krassovski, 2015) reaching  $0.4 \text{ m s}^{-1}$ . Our observations are  
 518 a finer-detailed representation of the kind of cross-shore transports inferred  
 519 by Mackas and Yelland (1999) from hydrographic surveys, and definitively show that this  
 520 water can originate from the shelf from relatively deep depths and be transported offshore.  
 521 We do not have velocity measurements for the water that replaces it, but assuming that  
 522 water also flows along-shelf, these separation events are associated with a large replacement  
 523 of shelf water with offshore water at this location. This emphasizes the importance of

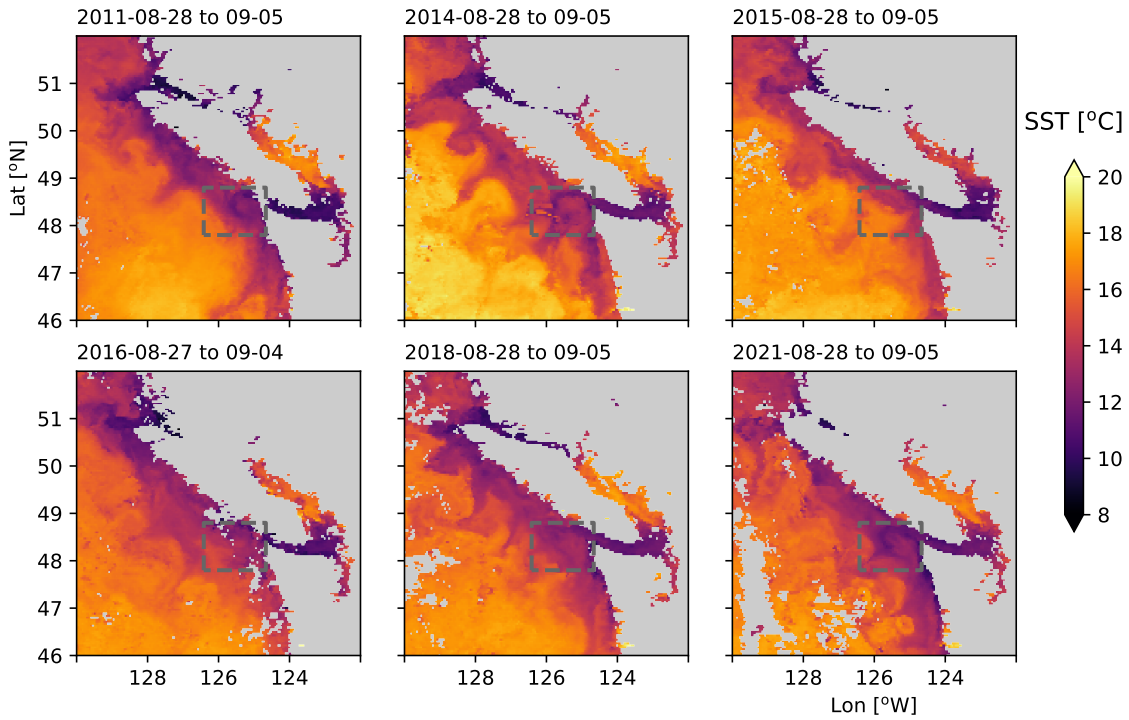


**Figure 16.** Available late-August sea-surface temperature from 8-day composites, 2011 to 2021 (NASA Ocean Biology Processing Group, 2019); missing years had too much cloud cover or no satellite coverage.

524 three dimensional observations and modeling of cross-shelf dynamics when thinking about  
 525 physical and biological processes on the shelf.

## 526 Open Research

527 Derived data files (1-m vertical binned CTD files) and analysis scripts are available at  
 528 <https://ocean-physics.seos.uvic.ca/~jklymak/PW13DataAnalysis/>. Raw CTD data  
 529 is available on request. Data was processed using a scientific python toolchain as listed at  
 530 <https://ocean-physics.seos.uvic.ca/~jklymak/PW13DataAnalysis/environment.yml>;  
 531 major components include xarray (Hoyer & Hamman, 2017), numpy (Harris et al., 2020),  
 532 and Matplotlib (Caswell et al., 2022), but those all leverage many smaller but vital projects.

## 533 Acknowledgments

534

535 Thank you to the officers and crew of the R/V Falkor and the Schmidt Foundation  
 536 for funding the seagoing component of the cruise. Thank you to Richard Dewey, Benjamin  
 537 Schieffe, and Rowan Fox for efforts during the cruise. [Jack Barth and an anonymous reviewer](#)  
 538 [provided valuable feedback on the manuscript](#). Klymak was supported by NSERC Discovery  
 539 grant RGPIN-2017-04050 and a Canadian Foundation for Innovation Leading Edge Fund  
 540 grant 36109, Allen was supported by NSERC Discovery grant RGPIN-105694-11, and Wa-  
 541 terman was supported by NSERC Discovery grant RGPIN-2020-05799.

## 542 References

- 543 Adams, K. A., Barth, J. A., & Chan, F. (2013). Temporal variability of near-bottom dis-  
 544 solved oxygen during upwelling off central Oregon. *J. Geophys. Res. Oceans*, 118(10),  
 545 4839–4854. doi: 10.1002/jgrc.20361
- 546 Barth, J. A., Pierce, S. D., & Smith, R. L. (2000). A separating coastal upwelling jet at  
 547 Cape Blanco, Oregon and its connection to the California Current system. *Deep Sea*  
 548 *Res. II*, 47(5–6), 783 - 810. doi: [http://dx.doi.org/10.1016/S0967-0645\(99\)00127-7](http://dx.doi.org/10.1016/S0967-0645(99)00127-7)
- 549 Batteen, M. L. (1997). Wind-forced modeling studies of currents, meanders, and eddies in  
 550 the California Current system. *J. Geophys. Res.*, 102(C1), 985–1010. doi: 10.1029/  
 551 96jc02803
- 552 Brink, K. (2016). Cross-shelf exchange. *Annu. Rev. Mar. Sci.*, 8(1), 59–78. doi: 10.1146/  
 553 [annurev-marine-010814-015717](#)
- 554 Castelao, R. M., & Barth, J. A. (2007, nov). The role of wind stress curl in jet separation  
 555 at a cape. *J. Phys. Oceanogr.*, 37(11), 2652–2671. doi: 10.1175/2007jpo3679.1
- 556 Caswell, T. A., Lee, A., Droettboom, M., De Andrade, E. S., Hoffmann, T., Klymak, J.,  
 557 ... Kniazev, N. (2022). *matplotlib/matplotlib: Rel: v3.6.0*. Zenodo. Retrieved from  
 558 <https://zenodo.org/record/7084615> doi: 10.5281/ZENODO.7084615
- 559 Connolly, T. P., Hickey, B. M., Geier, S. L., & Cochlan, W. P. (2010, mar). Processes  
 560 influencing seasonal hypoxia in the northern California current system. *J. Geophys.*  
 561 *Res.*, 115(C3). Retrieved from <https://doi.org/10.1029%2F2009jc005283> doi:  
 562 10.1029/2009jc005283
- 563 Dale, A. C., & Barth, J. A. (2001, jan). The hydraulics of an evolving upwelling jet flowing  
 564 around a cape. *Journal of Physical Oceanography*, 31(1), 226–243. doi: 10.1175/  
 565 1520-0485(2001)031(0226:thoaeu)2.0.co;2
- 566 D'Asaro, E. (1988). Generation of submesoscale vortices: A new mechanism. *J. Geophys.*  
 567 *Res.*, 93, 6685–6693.
- 568 D'Asaro, E. A., Shcherbina, A. Y., Klymak, J. M., Molemaker, J., Novelli, G., Guigand,  
 569 C. M., ... Özgökmen, T. M. (2018, Jan). Ocean convergence and the dispersion of  
 570 flotsam. *Proc. Natl. Acad. Sci. U.S.A.*, 201718453. doi: 10.1073/pnas.1718453115
- 571 Dewey, R. K., & Crawford, W. R. (1988). Bottom stress estimates from vertical dissipation  
 572 rate profiles on the continental shelf. *J. Phys. Oceanogr.*, 18, 1167–1177.
- 573 DFO. (2022). *Marine environmental data section archive, buoy c46206*. Ecosystem and  
 574 Oceans Science, Department of Fisheries and Oceans Canada. Retrieved 2022-01-31,  
 575 from <https://meds-sdmm.dfo-mpo.gc.ca>

- Dortch, Q., Rabalais, N. N., Turner, R. E., & Rowe, G. T. (1994, dec). Respiration rates and hypoxia on the Louisiana shelf. *Estuaries*, *17*(4), 862. doi: 10.2307/1352754
- Durski, S. M., & Allen, J. S. (2005). Finite-amplitude evolution of instabilities associated with the coastal upwelling front. *J. Phys. Oceanogr.*, *35*(9), 1606–1628. doi: 10.1175/jpo2762.1
- Engida, Z., Monahan, A., Ianson, D., & Thomson, R. E. (2016). Remote forcing of subsurface currents and temperatures near the northern limit of the California Current system. *J. Geophys. Res.*, *121*(10), 7244–7262. doi: 10.1002/2016jc011880
- Foreman, M. G. G., Callendar, W., MacFadyen, A., Hickey, B. M., Thomson, R. E., & Lorenzo, E. D. (2008). Modeling the generation of the Juan de Fuca Eddy. *J. Geophys. Res.*, *113*(C3). doi: 10.1029/2006jc004082
- Freeland, H., & Denman, K. (1982). A topographically controlled upwelling ceter off southern Vancouver Island. *J. Mar. Res.*, *40*(4), 1069–1093.
- Freeland, H., & McIntosh, P. (1989). The vorticity balance on the southern British Columbia continental shelf. *Atmosphere–Ocean*, *27*(4), 643–657.
- Harris, C. R., Millman, K. J., van der Walt, S. J., Gommers, R., Virtanen, P., Cournapeau, D., ... Oliphant, T. E. (2020, sep). Array programming with NumPy. *Nature*, *585*(7825), 357–362. Retrieved from <https://doi.org/10.1038/s41586-020-2649-2> doi: 10.1038/s41586-020-2649-2
- Hickey, B., Thomson, R., Yih, H., & LeBlond, P. (1991). Velocity and temperature fluctuations in a buoyancy-driven current off Vancouver Island. *J. Geophys. Res.*, *96*(C6), 10,507–10,538.
- Hoyer, S., & Hamman, J. (2017, apr). xarray: N-d labeled arrays and datasets in python. *Journal of Open Research Software*, *5*(1), 10. Retrieved from <https://doi.org/10.5334/jors.148> doi: 10.5334/jors.148
- Hu, C., Lee, Z., & Franz, B. (2012). Chlorophyll a algorithms for oligotrophic oceans: A novel approach based on three-band reflectance difference. *J. Geophys. Res.*, *117*(C1). doi: 10.1029/2011jc007395
- Ikeda, M., & Emery, W. J. (1984). A continental shelf upwelling event off Vancouver Island as revealed by satellite infrared imagery. *J. Mar. Res.*, *42*(2), 303–317. doi: 10.1357/00222408478502774
- Ikeda, M., Mysak, L. A., & Emery, W. J. (1984). Observation and modeling of satellite-sensed meanders and eddies off Vancouver Island. *J. Phys. Oceanogr.*, *14*(1), 3–21. doi: 10.1175/1520-0485(1984)014<0003:oamoss>2.0.co;2
- Klymak, J. M., Crawford, W., Alford, M. H., MacKinnon, J. A., & Pinkel, R. (2015). Along-isopycnal variability of spice in the North Pacific. *J. Geophys. Res.*, *2169*–9291. doi: 10.1002/2013JC009421
- Klymak, J. M., Shearman, R. K., Gula, J., Lee, C. M., D'Asaro, E. A., Thomas, L. N., ... others (2016). Submesoscale streamers exchange water on the north wall of the Gulf Stream. *Geophys. Res. Lett.*. doi: 10.1002/2015GL067152
- MacFadyen, A., & Hickey, B. M. (2010). Generation and evolution of a topographically linked, mesoscale eddy under steady and variable wind-forcing. *Cont. Shelf Res.*, *30*(13), 1387–1402. doi: 10.1016/j.csr.2010.04.001
- Mackas, D. L., Denman, K. L., & Bennett, A. F. (1987). Least squares multiple tracer analysis of water mass composition. *J. Geophys. Res.*, *92*(C3), 2907–2918.
- Mackas, D. L., & Yelland, D. R. (1999, nov). Horizontal flux of nutrients and plankton across and along the British Columbia continental margin. *Deep Sea Res. II*, *46*(11–12), 2941–2967. doi: 10.1016/s0967-0645(99)00089-2
- NASA Ocean Biology Processing Group. (2017). *MODIS-aqua level 3 mapped chlorophyll data version r2018.0*. NASA Ocean Biology DAAC. Retrieved from <https://oceancolor.gsfc.nasa.gov/data/10.5067/AQUA/MODIS/L3M/CHL/2018> doi: 10.5067/AQUA/MODIS/L3M/CHL/2018
- NASA Ocean Biology Processing Group. (2019). *MODIS-aqua level 3 mapped SST data version r2019.0*. NASA Ocean Biology DAAC. Retrieved from [https://oceandata.sci.gsfc.nasa.gov/ob/getfile/AQUA\\_MODIS](https://oceandata.sci.gsfc.nasa.gov/ob/getfile/AQUA_MODIS)

- 631 OSI SAF. (2015). *GHRSSST level 2p sub-skin sea surface temperature from the Advanced*  
632 *Very High Resolution Radiometer (AVHRR) on Metop satellites (currently Metop-A)*  
633 *(GDS V2) produced by OSI SAF.* NASA Physical Oceanography DAAC. Retrieved  
634 from [https://podaac.jpl.nasa.gov/dataset/AVHRR\\_SST\\_METOP\\_A-OSISAF-L2P-v1](https://podaac.jpl.nasa.gov/dataset/AVHRR_SST_METOP_A-OSISAF-L2P-v1)  
635 .0 doi: 10.5067/GHAMA-2PO02
- 636 Pelland, N. A., Eriksen, C. C., & Lee, C. M. (2013). Subthermocline eddies over the  
637 Washington continental slope as observed by Seagliders, 2003–09. *J. Phys. Oceanogr.*  
638 doi: 10.1175/JPO-D-12-086.1
- 639 Pierce, S. D., Allen, J. S., & Walstad, L. J. (1991). Dynamics of the coastal transition  
640 zone jet: 1. linear stability analysis. *J. Geophys. Res.*, 96(C8), 14979. Retrieved from  
641 <https://doi.org/10.1029/91jc00979> doi: 10.1029/91jc00979
- 642 Relvas, P., & Barton, E. D. (2005). A separated jet and coastal counterflow during upwelling  
643 relaxation off Cape São Vicente (Iberian Peninsula). *Cont. Shelf Res.*, 25(1), 29–49.  
644 doi: 10.1016/j.csr.2004.09.006
- 645 Sahu, S., Allen, S. E., Saldías, G. S., Klymak, J. M., & Zhai, L. (2022, mar). Spatial and  
646 temporal origins of the La Perouse low oxygen pool: A combined lagrangian statistical  
647 approach. *J. Geophys. Res.*, 127(3). doi: 10.1029/2021jc018135
- 648 Strub, P. T., Kosro, P. M., & Huyer, A. (1991). The nature of the cold filaments in  
649 the California current system. *J. Geophys. Res.*, 96(C8), 14743–14768. doi: 10.1029/  
650 91jc01024
- 651 Thomson, R. E., & Gower, J. F. R. (1998). A basin-scale oceanic instability event in the  
652 Gulf of Alaska. *J. Geophys. Res.*, 103(C2), 3033–3040. doi: 10.1029/97jc03220
- 653 Thomson, R. E., Hickey, B. M., & LeBlond, P. H. (1989). The Vancouver Island Coastal  
654 Current: Fisheries barrier and conduit. In R. J. Beamish & G. A. McFarlane (Eds.),  
655 *Effects of ocean variability on recruitment and an evaluation of parameters used in*  
656 *stock assessment models.* Fisheries and Oceans Canada.
- 657 Thomson, R. E., & Krassovski, M. V. (2015, dec). Remote alongshore winds drive variability  
658 of the California Undercurrent off the British Columbia–Washington coast. *J. Geophys.*  
659 *Res.*, 120(12), 8151–8176. doi: 10.1002/2015jc011306
- 660 Weaver, A. J., & Hsieh, W. W. (1987). The influence of buoyancy flux from estuaries  
661 on continental shelf circulation. *J. Phys. Oceanogr.*, 17, 2127–2140. doi: 10.1175/  
662 1520-0485(1987)017<2127:TIOBFF>2.0.CO;2